

Mapping of spectral species diversity in the Arctic tundra and its relationship with topographic complexity – a use case of the spectral species concept in biodiversity research and conservation

Marie-Lou Pijnenburg

Realized in the Spatial Ecology and Remote Sensing group, University of Zürich

Referee: Jake Alexander

Co-referee: Niklaus Zimmermann

External supervisor: Jakob Johann Assmann

Submission date: 13 November 2023

Table of Contents

<i>Abstract</i>	2
<i>1. Introduction</i>	3
<i>2. Material and methods</i>	5
<i>2.1 Study area and field data</i>	5
<i>2.2 Spectral data</i>	6
<i>2.3 Production of spectral species diversity maps</i>	7
<i>2.3.1 BiodivmapR parametrisation</i>	7
<i>2.3.2 AVIRIS-NG Sentinel-2 comparison</i>	7
<i>2.3.4 Principal component choice</i>	8
<i>2.4 Modelling the relationship between variation in topography and spectral species diversity</i>	8
<i>2.4.1 Data</i>	8
<i>2.4.2 Inla parametrisation</i>	8
<i>3. Results</i>	9
<i>3.1 The Sentinel-2-derived spectral species diversity was mostly homogeneously distributed</i>	9
<i>3.2 Higher spectral and spatial resolution influences spectral species diversity patterns</i>	10
<i>3.3 Topographic slope variation predicts spectral species diversity</i>	12
<i>4. Discussion</i>	13
<i>4.1 Sentinel-2 derived spectral species map captures tundra landscape diversity</i>	13
<i>4.2 Standard deviation of topographic slope predicted spectral species diversity at certain scales</i>	15
<i>4.3 The spectral species concept in the Arctic tundra, prospects and future directions</i>	16
<i>Conclusion</i>	17
<i>Acknowledgement</i>	18
<i>References</i>	19
<i>Supplementary material</i>	26

Abstract

The Arctic biome is changing rapidly, facing climate change and increased human activity. However, plant diversity response to these environmental modifications vary at the pan-Arctic scale and current knowledge is limited to few research sites in the vast Arctic tundra. Therefore, there is a need for more efforts to scale up the monitoring of plant communities and to understand the background mechanisms driving diversity patterns in the tundra, both of which can benefit from the use of remote sensing data. In this study, we used the spectral species concept and remotely sensed reflectance data to derive a spectral proxy for plant species richness over a 1200 km² area of the Canadian Arctic tundra (Cambridge Bay). The spectral species concept is based on the clustering of pixels with similar spectral signatures into so-called spectral species, from which diversity metrics can be computed over space and related to plant community diversity. We used Sentinel-2 multispectral and AVIRS-NG hyperspectral data at 10 and 5 m resolution, respectively, to explore the effect of spectral and spatial resolution on the spectral species diversity values. To illustrate the application of spectral species diversity in assessing the drivers of plant diversity, we modelled the relationship between spectral species diversity computed at different grain sizes and the variation in topographic slope and elevation, both expected to influence plant community through microclimate. The spectral species diversity from Sentinel-2 data differentiated between field sites with lower or higher in-situ plant species richness. However different patterns of spectral species diversity were output depending on the input data used. The variation in the topographic slope positively predicted spectral species diversity, while the variation of elevation did not. The relationship between topographic slope and spectral species diversity was stronger at 100 m and became weaker at larger grain size, breaking down at a grain size of 1 km. Our findings indicate the ability of the spectral species concept to differentiate between areas of Arctic tundra with varied plant diversity. Furthermore, the variation in topographic slope seems to be a useful predictor of spectral species diversity at 100 m resolution, in tundra landscapes similar to our study site. This could be due to its association with soil moisture. We believe this work will help improve monitoring of plant diversity at a larger spatial and temporal scale in the rapidly warming Arctic tundra landscape, and aid with conservation efforts that require the identification of biodiversity patterns and their drivers.

1. Introduction

Many aspects of the Arctic biome are rapidly changing due to direct and indirect impacts of human activities. Climate change has led to an increase in temperature which, at high latitudes, is nearly four times faster than the global average (Rantanen et al., 2022). This change in temperature regime drives permafrost thaw (Chadburn et al., 2017; Grosse et al., 2016) as well as changes in the precipitation and fire regime (Descals et al., 2022; McCrystall et al., 2021). Alongside, humans increased their direct influence on the Arctic tundra biome via expanded tourism and land use (Jaskólski, 2021; Runge et al., 2020). All direct and indirect human-induced changes affect the Arctic plant communities by altering their habitats.

The present-day Arctic plant diversity is highly driven by abiotic factors, which underlines its potential vulnerability to climate change (Iturrate-Garcia et al., 2016; Niskanen, Heikkinen, et al., 2017). The rough climatic conditions at high latitudes greatly shaped plant diversity and restricted the presence of many southern species, making it a generally vascular plant species poor environment (Daniëls et al., 2013; Murray, 1995). The Arctic tundra is however not a vast homogenous area, devoid of any lifeforms. The influence of climate can promote highly heterogeneous landscapes, where different plant communities cohabit on a very small scale (Daniëls et al., 2013; Ims et al., 2013; Nelson et al., 2021; Ponomarenko et al., 2019; Marilyn D. Walker et al., 2001). For instance, mesotopography can lead to patchy and diverse communities, as it affects soil moisture, snow cover, nutrient availability or wind exposition, and therefore microclimate (Nelson et al., 2021; Shaver et al., 1996). At a regional scale, higher temperatures or diversity in landscape features, such as the presence of an elevation gradient, can create diversity hotspots (Daniëls et al., 2013; Ims et al., 2013; Marilyn D. Walker et al., 2001). Considering the current state of Arctic plant communities, diversity patterns could change in different ways in the coming years, depending on the interaction of abiotic and biotic factors (Mod et al., 2016; Olofsson et al., 2013). For instance, plant diversity could increase due to the shift in distribution from species of southern latitudes, or decrease due to the homogenisation of the community through an overabundance of warm-loving species already present in the biome (Stewart et al., 2018; Marilyn D. Walker et al., 2001). However, current in-situ observations are limited and trends observed do not always align with these hypotheses (Bjorkman et al., 2020; Criado et al., 2023). A major challenge in the study of Arctic diversity lies in the spatially extensive and harsh nature of the biome, making fieldwork logistically challenging and field data acquisition without spatial biases difficult (Metcalfe et al., 2018).

Remote sensing can help overcome the many difficulties associated with collecting representative data over the large area of the Arctic, including data that allows for the estimation of plant diversity (Beamish et al., 2020). The acquisition and use of remotely sensed data, especially at higher spatial and/or spectral resolution, is continuously increasing (Beamish et al., 2020; Nelson et al., 2021). Different type of remotely sensed data presenting different spatial or spectral resolution can bring different benefits and challenges, making the choice of the data important and interesting to consider for answering different ecological questions (Beamish et al., 2020; Nelson et al., 2021; Yang et al., 2022). Remotely sensed reflectance data is however in many ways different from plant survey data (Rocchini, Torresani, et al., 2022). For instance, while remotely-sensed estimates of plant diversity might not be taxonomically as precise, it facilitates analyses linking biotic or abiotic components of the landscape to biodiversity due to its spatially explicit nature (Beamish et al., 2020; Nelson et al., 2021; Yang et al., 2022). Another advantage of using remote sensing compared to in-situ plant diversity data is the ability to scale the analysis in space and time more easily (Aplin, 2005; Beamish et al., 2020; Yang

et al., 2022). The use of remote sensing for the study of plant diversity patterns in the Arctic tundra and their causes is thus highly relevant and timely given the rapid environmental change in the biome.

To estimate plant diversity using remote sensing, we assessed the diversity of spectral signatures over space. The use of spectral diversity as a proxy for plant diversity rely on the spectral variation hypothesis, which states that higher spatial variation in the sensed spectra is associated with higher species richness, via higher environmental diversity (Palmer et al., 2002). Several measures of spectral variation or diversity can be used to apply the spectral variation hypothesis and thus serve as proxy for plant diversity (Gamon et al., 2020). In this study, we used the spectral species concept, originally developed for assessing tree diversity of a tropical forest. The spectral species concept is based on the segmentation of the spectral space into a pre-defined number of so called “spectral species” (Féret & Asner, 2014; Féret & de Boissieu, 2020). Pixels from remotely sensed data can then be clustered, based on the similarity of their spectral signature, and assign a spectral species. The diversity and abundance of spectral species observed over space can be used to compute diversity metrics, such as the Shannon index. As mentioned in Rocchini, Torresani, et al. (2022), the term spectral species can be confusing as each spectral species is not related to single species in the biological sense. However, the spectral species concept was not developed with the intention to exactly map each single taxonomic species, instead the term “species” simply refers to the grouping of similar pixels into a cluster, based on their spectral signature, akin to organisms sharing highly similar genetic code being grouped in taxonomic species (Féret & de Boissieu, 2020; Rocchini, Torresani, et al., 2022). This complicates the interpretation of a diversity metric calculated based on reflectance data from mixed pixels in respect to the taxonomic species diversity present in-situ. The presence of multiple plant species in a pixel can still affect its reflectance proportionally, but must not do so necessarily. Plant reflectance can for example be correlated with phylogeny and function rather than species identity (Schweiger et al., 2018). Furthermore, other aspects than species taxonomic identity influence reflectance data such as intraspecific variation in the water content of the plant, the health status of the plant, the presence of rocks or other non-vegetated surfaces in the pixel, or the presence of different phenological stages of the same species (Fassnacht et al., 2022; Rocchini, Santos, et al., 2022; Rocchini, Torresani, et al., 2022). Despite these limitations, the spectral species concept has been used to successfully map estimates of plant diversity in multiple studies and ecosystems (Gastauer et al., 2022; Kishore et al., 2023; Zhang et al., 2023).

In this study, we aim to produce a spectral species diversity map of the surroundings of Cambridge Bay (Nunavut, Canada) to identify patterns in plant diversity estimates and test their relationship with variation in topography. To this end, we used two different remote sensing datasets, multispectral data from Sentinel-2 satellites and hyperspectral data from NASA Arctic Boreal Vulnerability Experiment (ABOVE) campaign, at 10 and 5 m resolution respectively. The two datasets enabled us to explore the effect of higher spectral and spatial resolution on the resulting ability to capture diversity patterns. We hypothesize that the diversity estimates from the hyperspectral data differ from the multispectral data, as it contains more information, both spectrally and spatially. To illustrate the use of the spectral species concept in exploring the drivers of plant diversity, we investigated, using Bayesian hierarchical models, the relationship between variation in elevation as well as variation in topographic slope and the spectral species diversity index calculated for different window sizes. We hypothesize that higher spectral species diversity is linked to areas with higher variation in elevation and topographic slope, but we do not expect this relationship to hold true at all window sizes. To the best of our knowledge, our study is the first application of the spectral species concept in an Arctic terrestrial environment and therefore provides a unique opportunity to test the workflow for the study of plant diversity at high latitudes. We believe that the outcomes of this study will contribute to future

monitoring of plant diversity and to the understanding of the mechanisms driving tundra plant community diversity, in order to better understand how they will respond to climate change.

2. Material and methods

2.1 Study area and field data

Our study area is situated around Cambridge Bay, on Victoria Island, Canada and spanned a rectangular area of approximately 30 kilometres by 40 kilometres. The vegetation is comprised in the circumpolar bioclimatic subzone D, defined by the Circumpolar Arctic Vegetation Map, and dominated by erect dwarf shrub tundra and non-tussock sedge, dwarf-shrub, moss tundra (D. A. Walker et al., 2005). The Canadian High Arctic Research Station (CHARS), located in the community of Cambridge Bay, enabled Jakob J. Assmann and Debora S. Obrist, researchers from the Spatial Ecology and Remote Sensing group at the University of Zürich, to conduct fieldwork for their “Tundra eDNA project”, during the summer 2023. They shared the plant species richness data collected during this field season, in order to have in-situ data to work with for this project. Three different sites of 300 m² each, with visually different vegetation characteristics, were selected for data collection (Figure 1). Site 1 was located 1 km east of the town, site 2 was on the southwestern slope of the Ovayok territorial park esker and site 3 was on the east-facing slope of a sandy hill referred to as Mt. Augustus (Figure 1). They surveyed each site using 18 subplots where they recorded plant species presence, including moss and lichen species. As the smallest grain size used in our study (5 m resolution) is larger than the subplots (0.5 m radius), we could only compare the spectral species diversity with plant taxonomic diversity at the site level (Supplementary Figure S1). We defined the site-level species richness as the list of unique species from the cumulative species list of the 18 subplots (Supplementary table S1). The complete raw dataset is currently available from Jakob J. Assmann (jakob.assmann@uzh.ch) and will be made available in open access soon. Details about the fieldwork data collection can be found in the Supplementary method S1.

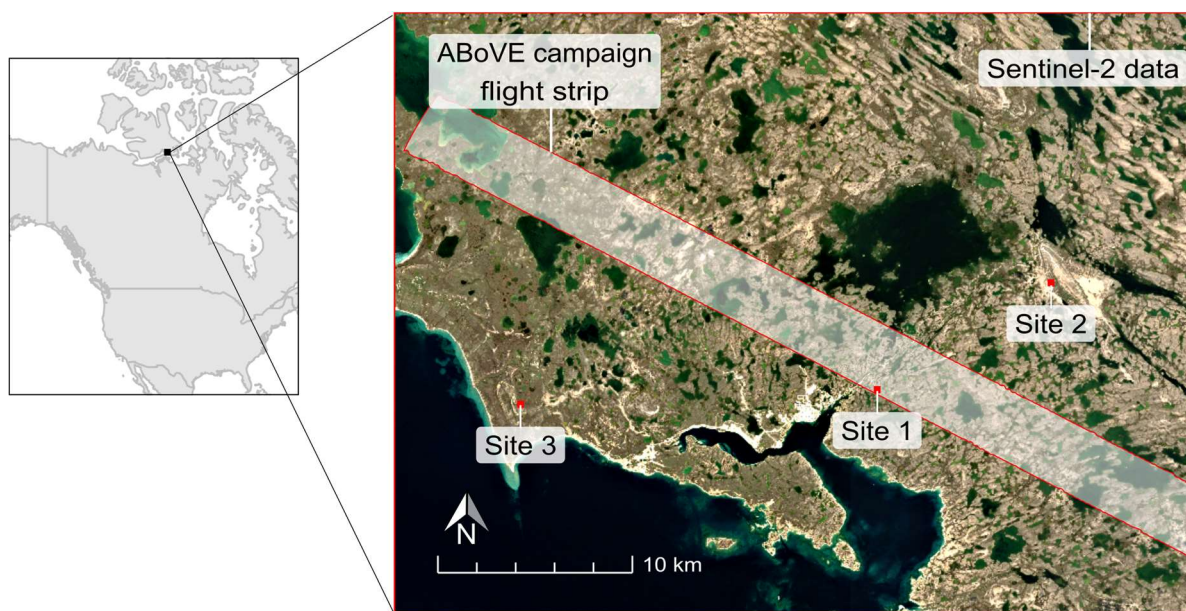


Figure 1: True colour map of our area of interest on Victoria Island, Cambridge Bay, Canada, produced from Sentinel-2 tiles. Site 1, 2, and 3 represent the location of the fieldwork site of the summer 2023. The boundary of the flight strip from the Arctic Boreal Vulnerability Experiment used in this study is represented in transparent white.

2.2 Spectral data

We identified and downloaded from the Copernicus Open Access Hub two cloud-free Sentinel-2 tiles to cover our area of interest, dated from the 27th of July 2019 (Copernicus Sentinel-2 (processed by ESA), 2021). One tile was already available as bottom of atmosphere reflectance (Level 2A) while the other had to be processed through the Sen2Cor ESA plugin to get Level 2A reflectance data from top-of-atmosphere (Level 1C) data (Main-Knorn et al., 2017). We then mosaicked and cropped them to the extent of our area of interest. Sentinel-2 data is multispectral and contains 13 bands, of which three are at 60 m resolution, six at 20 m resolution, and four at 10 m resolution (Copernicus Sentinel-2 (processed by ESA), 2021; Drusch et al., 2012). We disaggregated the 20 m resolution bands to 10 m resolution by bilinear interpolation, to keep ten bands to work with.

We used a second dataset with higher spectral and spatial resolution, collected during the Arctic-Boreal Vulnerability Experiment campaign of 2019 (Miller et al., 2022), to test the influence of different spectral and spatial resolution on the computation of spectral species diversity indexes. The data was collected by the AVIRIS-NG instrument at approximately 5 m resolution and covered the visible spectrum as well as the near-infrared and short-wave-infrared spectrum with 425 bands (5 nm spacing). Our area of interest over Cambridge Bay was covered by 15 flight strips of about 20 gigabytes each. However, due to the discrepancy between the flight strips data quality as well as the processing power it would require to process all 15 flight strips, we focused on one flight strip (ID: ang20190802t220708), covering 20% of our area of interest as well as one fieldwork site (Figure 1). The data needed to be rectified to be handled in R as a non-rotated object. To this end, we used `gdal_warp` which enabled us to rectify as well as to crop the input file to the extent of our area of interest (GDAL/OGR contributors, 2023).

We built masks for both datasets to remove pixels containing water, shade, cloud, and build-up area from the analysis. The water mask was based on the computation of the Normalized Difference Water Index (NDWI) (Gao, 1996). For Sentinel-2 data, it was calculated with the Near Infra-Red (NIR) band (842 nm) and the green band (560 nm). We set the cut-off for Sentinel-2 at 0.2 NDWI. The NDWI values for AVIRIS-NG data were computed by taking the average value of 20 bands between 800 and 900 nm for the NIR band and between 500 and 600 nm for the green band. We set the threshold at 0.1 NDWI, after assessment of the distribution of NDWI values. The shade mask was obtained by removing pixels with reflectance values in the NIR below the threshold of 1000 for Sentinel-2 and 0.05 for AVIRIS-NG data, following Féret & de Boissieu (2020) protocol, adjusted by visual assessment for best cut-off in our study system. Once again, the NIR value for AVIRIS-NG data was taken to be the average reflectance values of 20 bands between 800 and 900 nm. The mask for build-up area was created on the basis of an area of interest produced by Jakob J. Assmann for the “Tundra eDNA project”, which was constructed to exclude any buildings, roads or infrastructure and include a buffer zone of approximately 500 metres from these facilities as well as 5 km from the CYCB airport. As build-up areas were found along the coast, we masked all the pixels south of the area of interest from the “Tundra eDNA project” and kept the pixels north of it, as illustrated in the Supplementary Figure S2. Finally, the AVIRIS-NG flight strip contained some cloudy pixels which we removed as much as possible through a random forest pixel classification. The random forest algorithm was built with manually annotated cloudy and non-cloudy areas from four flight strips, including the one of interest. We included pixels from other flight strips than the one of interest as we initially intended to process more than one. For each annotated area, 10000 pixels were randomly extracted, resulting in a total of 70000 pixels included in the analysis. We used 70% of our data as training data and 30% as validation data and ran the random forest using the R function `randomForest()` (Liaw & Wiener, 2002). A first attempt at

obtaining spectral species diversity map over the AVIRIS-NG data resulted in a map with a large spot of low spectral species diversity. This was due to a cloud shadow that was not masked properly, highlighting the importance of data and mask quality to get meaningful results (Zhai et al., 2018). However, due to time constraints, we did not refine the randomForest cloud mask or the shade mask further. Instead, we manually cut out these areas in a GIS software, which added some subjectivity in the production of our mask. All separate masks were merged and applied to the data products.

2.3 Production of spectral species diversity maps

2.3.1 BiodivmapR parametrisation

Spectral species diversity maps were produced using the workflow designed in the biodivmapR R package, which was developed by the authors of the spectral species concept (Féret & de Boissieu, 2020). The main steps comprise a dimensionality reduction via principal component analysis (PCA), a k-mean analysis for pixels clustering based on spectral signature and the computation of a diversity map by looking at the diversity of spectral signatures in a window of predefined size. The k-mean analysis is internally iterated twenty times by the package function and the computation of diversity indexes based on the clustering data considers these distinct clustering outcomes.

We used identical general parameters to process Sentinel-2 and AVIRIS-NG data. The biodivmapR workflow gives the opportunity to filter pixels based on thresholding, a step we skipped as we already built masks separately (see above). The function to perform the PCA also offers to apply a continuum removal to normalize the reflectance spectrum. As this step is mentioned in Féret & de Boissieu (2020) as not to be of significant importance when pixels are larger than average plant size, we decided not to apply it, which also reduced our computation time. The dimensionality reduction was done through a scaled PCA and a second pixel filtering based on the PCA results was set to false. The number of 20 clusters for the k-mean analysis seemed more appropriate than the default setting of 50 clusters, as we are not capturing single plant species for each pixel, thus reducing the variety of potential landscape features. The AVIRIS-NG data did not have a resolution of exactly 5 m resulting in spectral species map of 5.099 m, which we resampled with a nearest neighbourhood algorithm to exactly 5 m. This added a small uncertainty to our data but was necessary to standardise the resolution of the output spectral species diversity map, and the resampling on the spectral species map was much less computationally intensive than if performed on the 425 bands of the AVIRIS-NG raw data. Finally, the window size to compute the Shannon index map was set to obtain maps of 100 m resolution, taking into account 10 by 10 pixels for Sentinel-2 and 20 by 20 for AVIRIS-NG. Additional Shannon index maps at 200 m, 300 m, 500 m and 1 km window sizes were subsequently computed to explore the link between spectral species diversity and topographic complexity across scale.

2.3.2 AVIRIS-NG Sentinel-2 comparison

To compare the results from AVIRIS-NG data to the results computed with Sentinel-2 data, we re-ran biodivmapR on a stretch of Sentinel-2 data covering only the area of the AVIRIS-NG flight strip. To this end, we resampled the AVIRIS-NG mask to 10 m resolution through nearest neighbourhood interpolation and masked the Sentinel-2 data with it. This enabled us to have the masked pixels in the AVIRIS-NG flight strip also masked in the Sentinel-2 view while still masking the pixels that had already been removed for the Sentinel-2 data. We computed correlation coefficients between the two spectral species diversity maps using the raster.modified.ttest() function from the SpatialEco R package (Evans Jeffrey, 2021). This function computes the correlation between rasters using a sliding window approach to account for spatial autocorrelation. We binned the resulting correlation coefficients to assess the area where the coefficients were at 0.5 or above, between 0 and 0.5 or negative.

2.3.4 Principal component choice

The biodivmapR developers mention the potential for some principal components (PCs) with little explained variance to still capture informative plant diversity data. To deal with those, they recommend a visual assessment of the PCs in a GIS software while considering previous knowledge about the studied area, to select those PCs showing patterns corresponding to known vegetation patterns. A first visual assessment of the Sentinel-2 PCs enabled us to identify five potentially informative PCs (PC 1,2,7,8 and 9). We then used the plant species richness data of the three fieldwork sites to choose the combination of PCs 1, 2, 7 and 8, which gave the best match between spectral richness and plant species richness. We obtained the spectral richness for each fieldwork site with the biodivmapR function `diversity_from_plots()` which computes richness and diversity index based on the number and distribution of different spectral signatures present in the area. We could not conduct a similar analysis with the flight strip of AVIRIS-NG data as it covers only one fieldwork site and we thus stuck to the visual assessment as suggested by the package authors. In this way, the PC 1 and 2 appeared to be informative. To input the same amount of information in further analysis between Sentinel-2 and AVIRIS-NG data, we decided to also keep PC 8 and 9, which appeared to be potentially informative. The other PC visibly captured noise.

2.4 Modelling the relationship between variation in topography and spectral species diversity

2.4.1 Data

The elevation and slope data over our area of interest was obtained from two tiles of the Arctic Digital Elevation Model (ArcticDEM) (Porter et al., 2023) at 2 m resolution (tile IDs: "29_21_1_" and "29_21_2_1"). We mosaicked and cropped the tiles to the extent of our area of interest. We used the `terrain()` function from the terra package to compute the topographic slope data from the elevation data. The standard deviation of elevation or topographic slope was then calculated using the `aggregate()` function for 100 m, 200 m, 300 m, 500 m and 1 km window sizes, matching the spectral species maps. However, the standard deviation of elevation increased with the mean of the elevation (Supplementary Figure S3) and the two are hence confounded. We expected this relationship to influence the hypothesised positive association between variation in topography and species spectral diversity. Indeed, due to the extreme conditions in the tundra around Cambridge Bay, increasing altitude is generally associated with lower plant diversity linked to a more exposed habitat and therefore harsher conditions (J.J. Assmann, personal communication, September 15, 2023). With the standard deviation of elevation confounded with the mean elevation, a higher standard deviation would mean higher mean elevation and therefore a lower expected plant diversity. We indeed observed a negative relationship between the Sentinel-2 derived spectral species diversity and the standard deviation of elevation (Supplementary Figure S3), which prompted us to use the coefficient of variation (CV) of the elevation as a topographic diversity measure instead, to account for the confounded relationship and solely focus on the relative variation in elevation. Due to low predictive power of the coefficient of variation in elevation to predict Sentinel-2 derived spectral species diversity, we only tested for the standard deviation of topographic slope as predictor of AVIRIS-NG derived spectral species diversity.

2.4.2 Inla parametrisation

A variogram analysis assessed the presence of spatial autocorrelation in our datasets (Supplementary Figure S4), which prompted us to use a statistical modelling method capable of accounting for it. To this end, we used the R INLA package (Bakka et al., 2018; Rue et al., 2017), which builds hierarchical models based on Bayesian statistics, where the posterior distributions are estimated through Laplace approximation. This method enables faster computation time than other Bayesian approaches (Bakka

et al., 2018; Rue et al., 2017). We built two independent models assessing the relationship between spectral species diversity and the variation in elevation or topographic slope, with the following formulas:

$$g(E(Y|X)) = \beta_0 + \beta_{\sigma(Slope)}X + \xi + \varepsilon$$

$$g(E(Y|X)) = \beta_0 + \beta_{CV(Elevation)}X + \xi + \varepsilon$$

With
 $g(\mu) = \log(\mu)$

Where g is the log-link function, $E()$ is the conditional mean function, Y is the Shannon index of spectral species values, X the predictor variable (either standard deviation in topographic slope or coefficient of variation in elevation), β_0 is the intercept, $\beta_{\sigma(Slope)}$ is the model slope for the standard deviation of topographic slope, $\beta_{CV(elevation)}$ is the model slope for the coefficient of variation of elevation, ξ is the latent field accounting for spatial effect, and ε is the residual error term which is expected to follow a Gaussian distribution. We fitted both models to our spectral diversity and topography data at different resolution to test the respective relationship across grain sizes. Our Shannon index data showed skewed-normal distributions. To address this, we configured our model with a gamma family distribution, which uses a log-link function in INLA. However, our datasets also included a few Shannon index values of 0, which are incompatible with the requirement of a strict positive distribution for the gamma distribution. To resolve this, we added one to our Shannon index values. We used the Matérn covariance function for the computation of the spatial autocorrelation between the non-masked pixels of our Shannon index raster. To assess the model fits, we plotted the observed Shannon index values against the fitted ones and computed pseudo-R² values following the equation in Vollenweider et al. (n.d.). We considered coefficient estimates to be significant when 95% of their posterior distribution lies outside of the null value, zero in our case (Kruschke, 2018). All the code written for this project can be found under the following repository:
<https://github.com/pijnenburgml/master-thesis>

3. Results

3.1 The Sentinel-2-derived spectral species diversity was mostly homogeneously distributed

We observed a mostly homogeneous distribution of spectral diversity around Cambridge Bay in our Sentinel-2-derived Shannon diversity map at 100 m resolution (Figure 2). There was still some variation in the map, which was particularly noticeable at location of lower spectral diversity – for instance in the upper left corner of the area of interest (Figure 2). The different combinations of PCs, made from the pre-selected informative PCs, resulted in a noticeable variation in the outputted Shannon index values (Supplementary Figures S5 and S6). With the chosen combination of PC 1, 2, 7 and 8, field site 3 could be distinguished as being more diverse than the others and field sites 1 and 2 as being equally diverse (Supplementary Figure S5). Nonetheless, the spectral species diversity always underestimated the plant diversity observed at the field sites (Supplementary Figures S5 and S6).

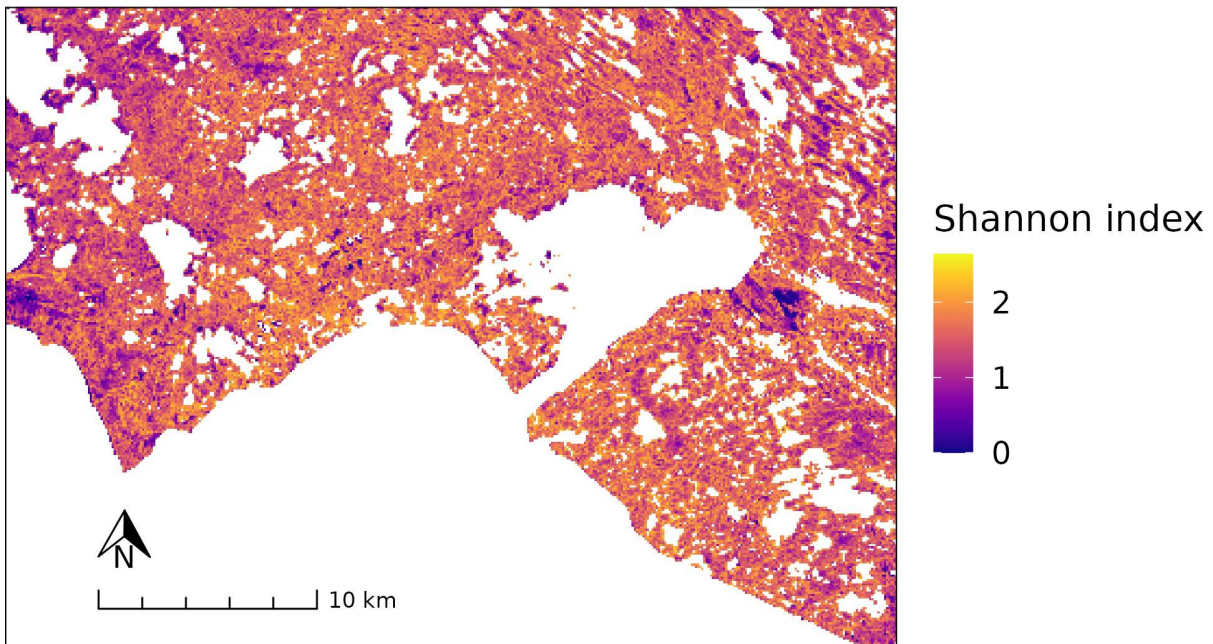


*Figure 2: Shannon index of spectral diversity around Cambridge Bay based on the Sentinel-2 satellite image. The diversity index was calculated at a 100 m resolution, using the *biodivmapR* workflow. The diversity of spectral signature was determined via a k-mean clustering of pixels, after dimensionality reduction of the Sentinel-2 derived bottom of the atmosphere reflectance values (L2A product).*

3.2 Higher spectral and spatial resolution influences spectral species diversity patterns

The spectral Shannon index map computed on one flight strip of AVIRIS-NG data showed different patterns than the corresponding map computed from Sentinel-2 data (Figures 4B and 4C). Both maps mainly showed Shannon index values ranging between 1 and 2, but spots of lower diversity index values were found at different locations. Hence, the computation of a correlation coefficient between the AVIRIS-NG and Sentinel-2 derived maps presented a considerable area where the Shannon index values were only weakly correlated or negatively correlated (Figure 4D). Approximately 66% of the flight strip area had a correlation coefficient between 0 and 0.5 and for approximately 7% of the area this value was below 0.

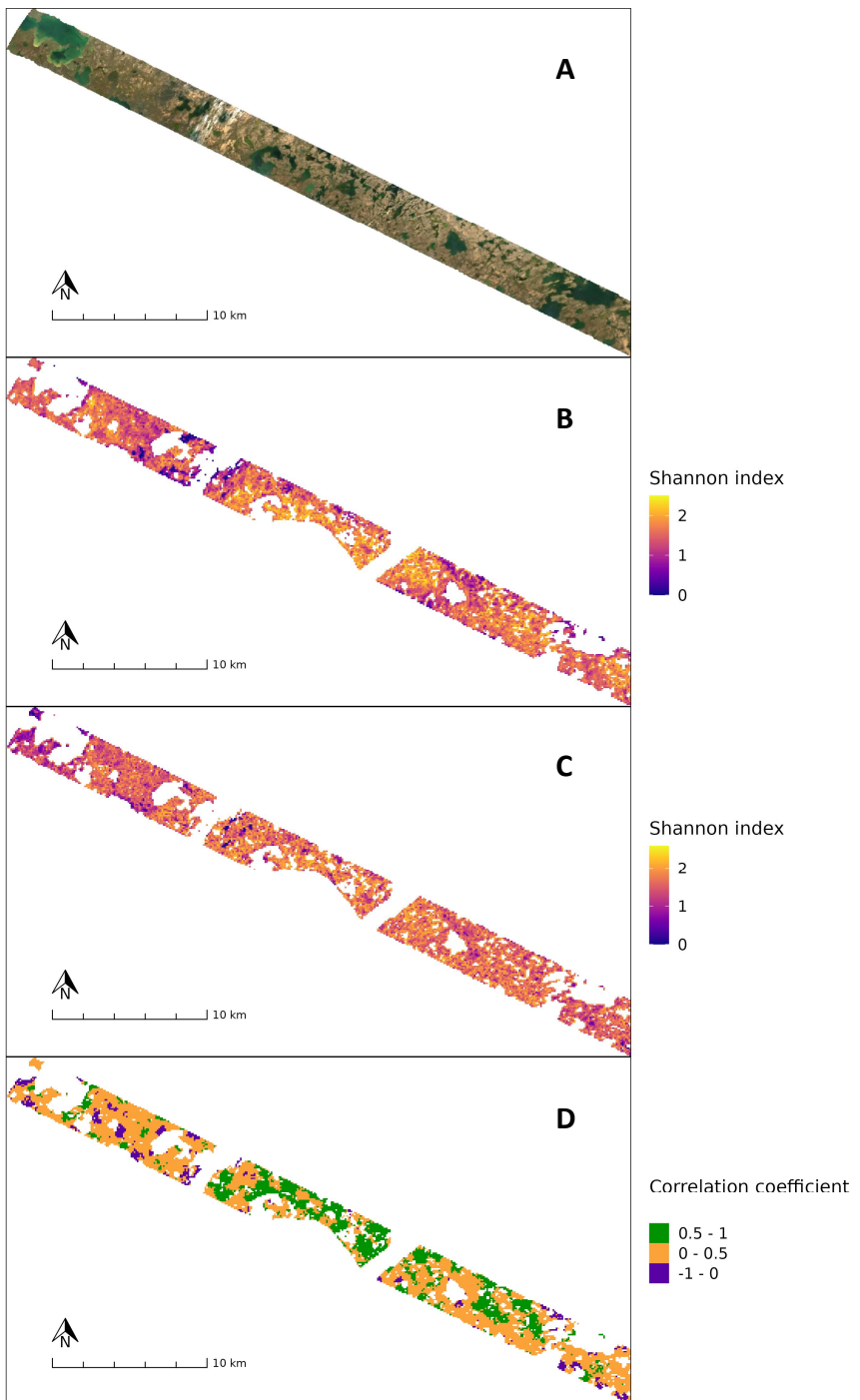


Figure 3: Effect of higher spatial and spectral resolution on the computation of spectral diversity maps with the biodivmapR package. A) True colour image of the flight strip from the Arctic Boreal Vulnerability Experiment (ABoVE). B) Shannon index of spectral species diversity map computed from the hyperspectral ABove data through the biodivmapR package. The ABove raw data is collected with the AVIRIS-NG instrument at a 5 m spatial resolution and comprises of 425 narrow spectral bands at 5 nm spacing C) Shannon index of spectral species diversity map computed from multispectral Sentinel-2 data with the biodivmapR package. Sentinel-2 raw data comprises of 10 broad spectral bands at 10 m spatial resolution. D) Map of correlation coefficients between Shannon indexes computed from AVIRIS-NG data and Sentinel-2 data. The correlation coefficient was computed taking into account spatial autocorrelation. Correlation coefficients were binned in three groups: negative, between 0 and 0.5, above 0.5.

3.3 Topographic slope variation predicts spectral species diversity

We found a positive relationship between the standard deviation of the topographic slope and the spectral diversity computed from the Sentinel-2 image, especially at 100 m resolution (Figure 3, Supplementary Table S2). The effect size of the relationship between standard variation in topographic slope and spectral diversity declined with increasing grain size and became insignificant for grain sizes over 500 m (Figure 3, Supplementary Table S2). The best fitting model was also the one computed at 100 m resolution, with a pseudo- R^2 of 0.8 (Supplementary Figure S7). However, the model fit could still be improved for all the models, as the plots of the input Shannon index values against the model fitted Shannon index values showed that these were underestimated or overestimated at the range limits (Supplementary Figure S7 and Figure S8). The model coefficient estimates of the CV of elevation were non-significant at all grain sizes (Figure 3, Supplementary Table S3). The range output from the models was in the same span as the range estimated through our semi-variograms (Supplementary Figure S4, Supplementary Table S2 and Table S3).

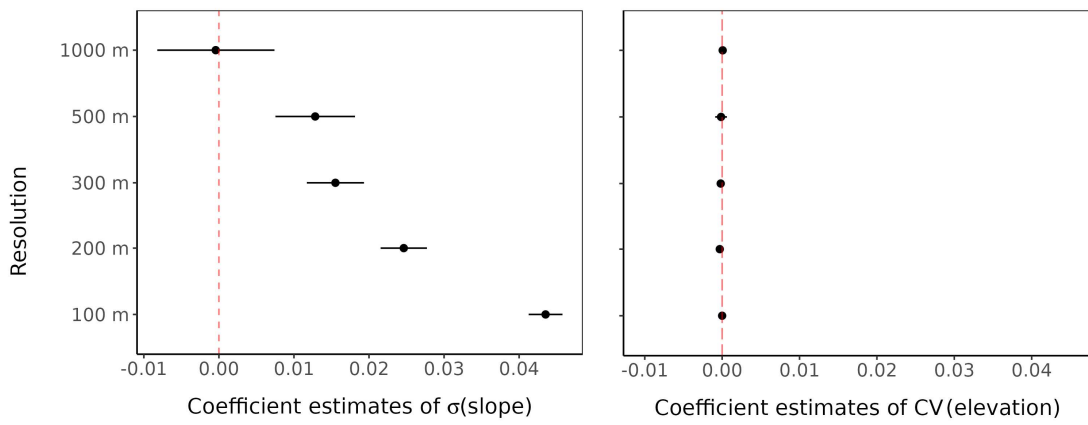
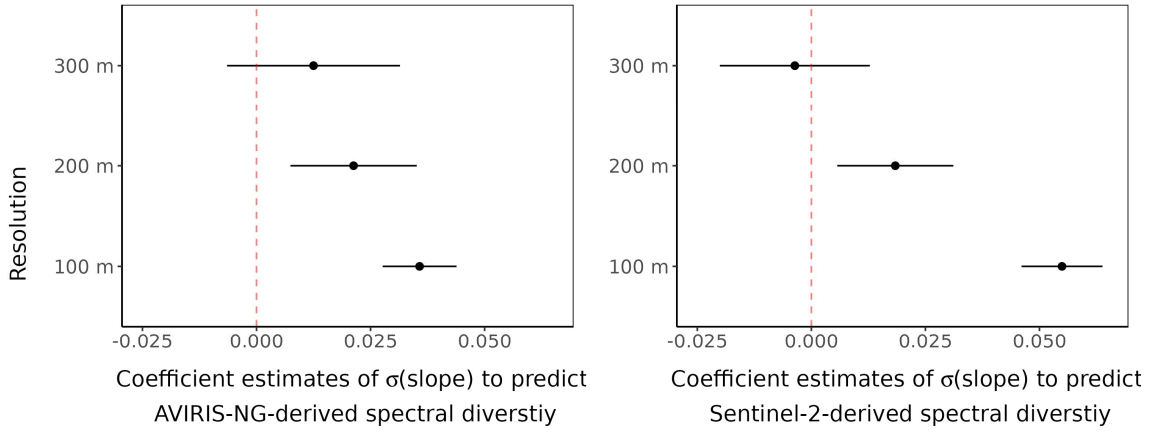


Figure 4: Model coefficients of the standard deviation in slope (left) and coefficient of variation in elevation (right), coming from independent models built with the INLA R package, explaining the spectral species diversity computed with the Shannon index over an area of interest. Models were run with spectral species diversity and variation in slope or elevation over 100, 200, 300, 500, or 1000 m resolution. The point is the mean and the bars are the 95% confidence interval of the posterior effect size distribution.

The coefficient estimates of the standard deviation in topographic slope to predict AVIRIS-NG-derived Shannon index values were slightly smaller than the ones from models computed with Sentinel-2 data, but were also positive and significant at 100 m and 200 m resolution (Figure 5, Supplementary Table S4 and Table S5). The relationship was not significant at 300 m or above, for both AVIRIS-NG and Sentinel-2 data (Figure 5, Supplementary Table S4 and Table S5). The pseudo- R^2 values from the model computed with the AVIRIS-NG data at 100 m (pseudo- $R^2=0.92$) was however higher than the one from the model computed with the Sentinel-2 data (pseudo- $R^2=0.76$). This held true at larger grain size (Supplementary Figure S9 and S10).



*Figure 5: Model coefficients of the standard deviation in topographic slope for explaining the spectral diversity in hyperspectral data (left) and multispectral data (right) computed over the same area of interest. Spectral diversity was defined with the *biodivmapR* package, which computes Shannon index of spectral species over specified window size. The hyperspectral data came from the Arctic Boreal Vulnerability Experiment and were collected using the AVIRIS-NG instrument at a 5 m spatial resolution with 425 bands with 5 nm spacing. The multispectral data came from the Sentinel-2 satellite, which collects 10 broad spectral bands at 10 m resolution. Models were run with both predictor and response computed at 100 m, 200 m, and 300 m resolution. The points represent the mean posterior effect size estimates and the bars the 95% confidence intervals of the posterior effect size.*

4. Discussion

We could show that the spectral species concept and associated *biodivmapR* workflow, initially developed for tropical forest landscapes, also has potential for applications in Arctic tundra environments. The Sentinel-2 map of spectral species diversity around Cambridge Bay could, under specific parametrisation, distinguish the fieldwork sites by their level of species richness. The use of data with a higher spectral and spatial resolution led to different patterns of spectral species diversity, although we were unable to determine whether these plant richness estimates were more or less accurate due to the lack of replicated field observation in the sub-section of the area of interest for which the hyperspectral data was available. Interestingly, we did not find a relationship between the variation in elevation and our spectral species diversity Shannon index. However, the variation in topographic slope predicted spectral species diversity positively. This effect was scale dependent and we observed the largest effect size and explanatory power of the model at 100 m resolution. Based on these results, we conclude that the spectral species concept is a promising framework that could help assist biodiversity monitoring and conservation efforts in the tundra, but further validation is required. Moreover, the ability of the topographic slope to predict spectral species Shannon index can be due to its association with soil moisture and represents an encouraging result for future use of the workflow to explore drivers of plant diversity in the Arctic tundra.

4.1 Sentinel-2 derived spectral species map captures tundra landscape diversity

Our map of spectral species diversity indicates an overall homogenous tundra landscape, which is in line with previous observations of the plant community surrounding Cambridge Bay. Findings from others studies report that the tundra landscape around Cambridge Bay varies at a small scale without exhibiting substantial heterogeneity at larger scales (Ponomarenko et al., 2019; Saarela et al., 2020). For instance, the high-resolution plant community map by Ponomarenko et al. (2019) that covers an

area of ~50 km² north of Cambridge Bay, shows the dominance of the “Mountain-avens – Single-spike sedge” community across the area, which the authors described as spectrally stable in space. We suppose that the presence of such a matrix community with a stable spectral signature across space, combined with small patches of other plant communities below 100 m² (the grain size of our maps), is likely to drive the Shannon index to intermediate values, typically falling between 1 and 2 (Strong, 2016). Amongst the generally homogeneous spectral species diversity, we also observed some scattered areas with lower spectral species diversity values. These could represent particularly homogenous areas, spectrally stable over space, of plant communities or non-vegetated ground. Despite the overall homogeneity of our map, comparison of smaller areas can reveal small difference in spectral species richness.

The ranking of the three fieldwork sites according to their spectral species richness matched the ranking of the taxonomic richness in the in-situ observation. Specifically, the spectral species richness values distinguished the fieldwork site 3 as more diverse than the others, and site 1 and 2 as equally diverse. However, we lacked sufficient in-situ data to statistically assess the relationships between Sentinel-2 derived spectral species and the ground-based plant taxonomic diversity across the area of interest. As data collection in the Arctic is difficult, Beamish et al. (2020) highlighted the need for scientific collaboration to increase the sharing of datasets, which would typically be of particular interest to help assessing accuracy of remote sensing studies. Furthermore, spectral species richness always underestimated taxonomic richness in our study. A result that we expected as we limited the number of possible spectral species to 20 since mixed pixels do not capture single species but rather part of a plant community. A larger number of field sites could have enabled us to find a linear factor to correct for the underestimation of the spectral species diversity, as suggested in Féret & Asner (2014). The underestimation of plant diversity by spectral species diversity is often reported in the literature, but research has shown that it can still translate to good prediction of plant species diversity overall (Féret & Asner, 2014; Gholizadeh et al., 2020; Kishore et al., 2023; Liccari et al., 2022; Rossi et al., 2021; Zhang et al., 2023).

The influence of the different combinations of PCs as well as the choice of the input data source had a notable effect on our spectral species estimates and both should therefore be considered when planning future work. The considerable influence of the choice of the PCs on the downstream k-mean clustering supports the statement of Féret & de Boissieu (2020), that choosing PCs simply based on their percentage of variance explained can lead to sub-optimal results. However, the choice of the PCs in the biodivmapR workflow is supposed to be done solely on the basis of a visual interpretation of the data in a GIS software, leaving the researcher to make a subjective decision (Féret & de Boissieu, 2020). We therefore carried out additional analysis to find the PCs combinations that best represented the in-situ data and suggest future studies to do so likewise. The input data had a similarly large influence on the spectral species diversity values. The use of AVIRIS-NG or Sentinel-2 data affected the pattern of spectral species diversity, not only in the strength but also in the direction of change of diversity values over space, as shown by the small or negative correlation coefficient values. In a tropical context, Kishore et al. (2023) found higher accuracy in their spectral species diversity computed from AVIRIS-NG data compared to Sentinel-2 data. The lack of replicated in-situ plant diversity data within the flight strip from the ABoVE campaign prevented us from assessing if this observation also holds true for our area of interest and future work is needed to address this question.

The additional information provided by the higher spectral and spatial resolution of the AVIRIS-NG data could potentially allow for more accurate estimates of tundra plant diversity patterns compared to the coarser Sentinel-2 data, but in this study, these potential benefits were outbalanced by the complications linked both to the use of AVIRIS-NG data and the biodivmapR workflow. First, a higher

spectral and spatial resolution could require a higher number of clusters as input for in the k-mean algorithm, leaving more room for subjective error when making comparisons between datasets, something not commented on by Kishore et al. (2023). Additionally, the many flight strips from the ABoVE campaign showed large discrepancies in data quality, thus limiting our analysis to only one of them, as we could not produce a cross-calibrated multi-flight strip mosaic within the timeframe of this project. This data quality issue questions the reliability of this dataset, compared to the well cross-calibrated Sentinel-2 product and associated quality control (Drusch et al., 2012; Main-Knorn et al., 2017; Phiri et al., 2020). The greater computing power required to handle the large amount of data produced by the AVIRIS-NG instrument also favours the use of the multispectral data. A further benefit of the Sentinel-2 data is the ability for scaling up the spectral species diversity assessments in time and space thanks to the high return rate of Sentinel-2, which increases the likelihood of cloud-free scenes (Drusch et al., 2012) – often a limiting factor in the Arctic (Myers-Smith et al., 2020). However, the continuous development of satellite missions using hyperspectral instruments coupled with improved computing algorithms (Beamish et al., 2020; Qian, 2021; Rast et al., 2021; SK & S, 2024) could change the overall balance of costs and benefits between the two data types, disfavouring the use of multispectral Sentinel-2 data compared to hyperspectral data for spectral species diversity mapping in the future.

4.2 Standard deviation of topographic slope predicted spectral species diversity at certain scales

Variation in topographic slope, but not variation in elevation, significantly explained spectral species diversity in our study, which could be due to the link between topographic slope and soil moisture, a factor that has been shown to be important in defining Arctic tundra plant communities. The variation in topographic slope and elevation differs in the information content they provide. For instance, if variations in small-scale topography are abundant across a relatively flat area, the standard deviation in slope can be high despite the standard deviation in elevation being low. As such, the standard variation in slope may provide more information about topographic complexity than the variation in elevation, especially in relatively flat landscape such as the observed one around Cambridge Bay. Although less commonly found in ecological studies than variation in elevation, the standard deviation of topographic slope has already been shown to explain plant diversity in a range of environments (Ceballos et al., 2015; Everson & H. Boucher, 1998; Yu et al., 2015). Moreover, in the Sub- and High-Arctic, topographic slope is closely linked to soil moisture, which is an important predictor of plant community types (Dearborn & Danby, 2017; Jedrzejek et al., 2013; Niskanen, Luoto, et al., 2017). Thus, the ability of the topographic slope to predict spectral species diversity aligns with the hypothesized link between spectral species diversity and plant community diversity. Furthermore, Dearborn & Danby (2017) conclude that differences in elevation affect soil moisture to a lesser extent than topographic slope, which could partly explain the lack of explanatory power in the variation of elevation for predicting spectral species diversity.

The scale dependence observed in our model exploring the relationship between spectral species diversity and topographic slope is consistent with our hypothesis and highlights the need to consider grain size when linking spectral species diversity with other variables. Above 500 m grain size, the variation in topographic slope no longer predicted Sentinel-2 derived spectral species diversity. This could be due to the homogenisation of one of the two features as the number of pixels taken into account for their computation increases, leading to a loss of signal in the expected relationship between topographic complexity and spectral species diversity. The fact that the relationship breaks down with larger grain sizes is consistent with other studies findings, suggesting plant species diversity and topography to be particularly dependent on smaller spatial grains rather than larger spatial grains in environments presenting harsh climatic conditions (He et al., 2006; Polyakova et al., 2016). However,

although the relationship between environmental heterogeneity and species diversity has been repeatedly shown to depend on spatial grain size and extent (e.g Crawley & Harral, 2001; Stein et al., 2014), the exact way in which scale affects the relationship can vary, and higher correlations between topographic complexity and plant species have also been observed with larger grain sizes (Yu et al., 2015). This highlights the potential for the observed scale dependence in the relationship between standard deviation in topographic slope and spectral species richness to be specific to our study system. Additionally, the measures used to define environmental heterogeneity should also influence the scale-dependent relationship with species diversity, as different processes might explain plant diversity at different scales (Crawley & Harral, 2001; Lundholm, 2009; Tamme et al., 2010; Tsamba et al., 2023). For instance, the lower spectral species diversity observed in the upper left corner of our map could be explained by other factors than topographic variation. Indeed, it is an observation that still holds at larger grain size while the topographic slope variation does not predict spectral species diversity anymore at grain size larger than 500 m. Further research, including at larger spatial extent, would probably help to understand this observed trend. Our statistical modelling results from the comparison between spectral species diversity data derived from the AVIRIS-NG flight strip and the corresponding Sentinel-2 subset also indicate a scale dependence, where the standard deviation in topographic slope no longer predicts spectral species diversity at 300 m resolution. All in all, our findings indicate that distances of approximately 100 m would make a good grain size for remote sensing studies of the Arctic tundra vegetation in environments similar to Cambridge Bay and its surroundings.

4.3 The spectral species concept in the Arctic tundra, prospects and future directions

An accuracy assessment including additional field data, as well as an upscaling of the analysis in space and time would help to further evaluate the use of the spectral species concept, through the biodivmapR workflow, in the Arctic tundra for the study of plant diversity patterns. A larger set of in-situ plant diversity data would enable a better assessment of the accuracy of the spectral species diversity maps and allow for the estimation of the statistical relationship between spectral species diversity and taxonomic species diversity in the Arctic tundra ecosystem similar to our study system. Several datasets around Cambridge Bay exist and could be used to this end (e.g. Ponomarenko et al., 2019; Saarela et al., 2020), but none are publicly available at the time-point of this study. Alternatively, additional field campaigns could be conducted around Cambridge Bay, or our analysis could be replicated for other tundra areas where more in situ data is available. The implementation of the biodivmapR workflow over other studied Arctic tundra sites would also help evaluate the applicability of the method across the varied ecosystems in the biome. Indeed, several studies advise caution on using the spectral variation hypothesis to estimate species diversity as it was found to be influenced by habitat type, alongside seasonality or window extent (Fassnacht et al., 2022; Michela et al., 2023; Schmidlein & Fassnacht, 2017; Van Cleemput et al., 2023). To the best of our knowledge, so far no other study has evaluated how well the spectral variation hypothesis, through the spectral species concept, holds in Arctic tundra habitat types. The plot network of the International Tundra Experiment (ITEX) could potentially be used to assess this further, as the species diversity knowledge over these study sites is already extensive (Criado et al., 2023; Henry et al., 2022). Furthermore, as phenology can have a strong influence on remotely sensed spectra (Beamish et al., 2020; Fassnacht et al., 2022; Nelson et al., 2021; Rocchini, Torresani, et al., 2022; Schmidlein & Fassnacht, 2017), we suggest future studies to test the integration of several image scenes taken across the growing season, for instance, such as done by Liccari et al. (2022) in a temperate ecosystem. In the Arctic, remote sensing of the vegetation just after snow melt or just before the first snow fall could help the detection of lichen and moss diversity (Nelson et al., 2021). The reliability of the spectral variation hypothesis also depends on the method used to define spectral diversity within an area. Some of the most common methods involve the computation of the volume or area of the convex hull in the spectral or principal component space, the coefficient of variation of reflectance data, or the variation of a vegetation index

(Gamon et al., 2020; Michela et al., 2023; Rossi et al., 2022; Schmidlein & Fassnacht, 2017). However, we are confident in the use of the biodivmapR package, or comparable approaches, to estimate plant diversity as several studies showed its better ability to capture the spectral variation hypothesis (Fassnacht et al., 2022; Rossi et al., 2022; Schmidlein & Fassnacht, 2017). The reason for this may be related to the use of categorical data (e.g. spectral species) to calculate the diversity metric rather than continuous data (e.g. coefficient of variation values), which should limit the influence of extreme pixels, as suggested by Fassnacht et al. (2022). Finally, following the results of Van Cleemput et al. (2023), and akin to our scaling analysis for the topographic variation – spectral species diversity relationship, we encourage testing for different window sizes to find which one enables the spectral variation hypothesis to hold.

Once the limitations of its applicability assessed, the spectral species concept could benefit biodiversity monitoring, research and conservation in the Arctic tundra. The biodivmapR workflow has been useful in the evaluation of the rehabilitation status of mines in tropical forests (Gastauer et al., 2022) and similar use cases could be found in the Arctic tundra where mining is also of importance, causing soil erosion and the spread of acidic or metallic elements in the terrestrial ecosystems (Tolvanen et al., 2019). Monitoring mined areas represents a costly process (Amirshenava et al., 2021; Gastauer et al., 2022), especially in the remote Arctic, making remote sensing-based monitoring particularly attractive. The evaluation of the rehabilitation status of an ecosystem through the use of the spectral species concept could potentially be extended to various other types of disturbances occurring in the tundra, such as post-fire vegetation recovery or other human-made disturbance associated with oil fields (Beamish et al., 2020; Heim et al., 2021; M. D. Walker, 1995). Moreover, the absence of pan-Arctic trends in diversity change (Criado et al., 2023) emphasizes the importance of broader-scale monitoring for a better understanding of the ongoing transformation of Arctic tundra plant communities in response to global warming (Metcalfe et al., 2018; Virkkala et al., 2019). The increase in abundance of certain species already observed in some locations, such as shrub or thermophile graminoid species (Bjorkman et al., 2020; Elmendorf et al., 2015), could be detected through a reduction in spectral species diversity over time, helping monitoring of homogenisation for example. As done in this study, spectral species diversity can also be correlated with abiotic drivers, to explore potential mechanisms associated with observed patterns of spectral species diversity. The difference in growing degree days, the topographic wetness index, snow persistence, nutrients availability, and/or bedrock substrate could all explain variation in species richness and thus be linked to spectral species diversity as well (McKane et al., 2002; Niskanen, Heikkinen, et al., 2017; Rissanen et al., 2023). Such applications of monitoring of spectral species diversity could also help identify locations for sites of interest for further field research, thereby reducing spatial biases in Arctic studies and aiding with logistical planning.

Conclusion

In this study, we applied the spectral species concept for the first time in an Arctic tundra landscape and leave a blueprint for similar mapping of spectral diversity baseline in the biome. Our findings highlight the potential of the method for plant diversity monitoring in the tundra when parametrised appropriately, but also show that further research is needed to establish best practices for the implementation of the workflow. With such efforts, we believe that the resulting spectral diversity maps can help biodiversity conservation and monitoring in the tundra, thereby benefiting research and land management efforts at a large scale. Furthermore, our findings also showed that spectral species diversity was predicted by the variation in topographic slope in our study system up to 500 m resolution. This lends support to the ability of spectral species diversity to act as a proxy of plant community diversity, as plant community in the tundra is shown to be positively linked to topography via soil moisture. Conducting additional research on the association of other factors with spectral

species diversity across various locations in the Arctic could help better constrain the diverse drivers responsible for the variation in changes of plant diversity at a circumpolar scale. We also showed that the relationship between spectral species diversity and abiotic variables are scale dependent, making it important to consider several scales for future studies. Overall, we therefore believe that the application of the biodivmapR workflow and the associated spectral species concept could provide a pathway to address some of the important gaps in terrestrial Arctic biodiversity research.

Acknowledgement

I would like to thank the Spatial Ecology and Remote Sensing group for welcoming me for this project. Especially, Jakob J. Assmann for all his wise advice and feedbacks all along the project, always given with kindness, but also for providing the fieldwork data from his “Tundra eDNA project”. I would also like to thank Debora Obrist who agreed as well to share the data collected in the fieldwork of summer 2023. I particularly appreciated the help of Ramona J. Heim for the comprehension of the R-INLA package. I would also like to acknowledge the feedbacks on my thesis draft from Gabriela Schaeppman-Strub. Finally, I especially value the time taken by my friend Julian Rieder to do a final proofreading. As the in-situ plant observation data from Cambridge Bay, Nunavut, Canada were collected by Jakob Assmann and Debora Obrist in summer 2023, the project team would like to thank the people of the Kitikmeot for the opportunity to conduct research on their land. The “tundra eDNA project” received funding from the Swiss Polar Institute (grant number SPIEG-2022-001) with supplementary funding and support from Prof. Dr. Gabriela Schaeppman-Strub and the Spatial Ecology and Remote Sensing Group at the University of Zurich, Switzerland. The field research was conducted under the umbrella of the following permits and licenses: Nunavut Research License (No. 04 023 23N-A), Kitikmeot Inuit Association Land-Use Certificate of Exemption: (KTX123X017), Nunavut Wildlife Research Permit (2023-042) and the Nunavut Territorial Parks Use Permit (2023-01 PU). Logistical and research support for the project was provided in-kind by POLAR Knowledge Canada and the Canadian High Arctic Research Station (CHARS) in Cambridge Bay. The project team would like to give their special thanks to the whole CHARS team for their support, to Erin Cox for her generous help and contributions to the research and logistics, to Nicolas Nantel-Fortier and Martin Leger for coordinating the lab use at CHARS, to Gilda Varliero and Beat Frey for their input on sampling design and planning of the logistics, to Jesse Jorna for spontaneous field support, to Meredith Christine Schuman for loaning the dGNSS devices and to the community of Cambridge Bay for welcoming the field team so warmly during their stay.

References

- Amirshenava, S., Osanloo, M., & Esfahanipour, A. (2021). Development of open-pit mine reclamation cost estimation models: A regression based approach. *International Journal of Engineering*, 34(11), 2467–2475. <https://doi.org/10.5829/ije.2021.34.11b.10>
- Aplin, P. (2005). Remote sensing: Ecology. *Progress in Physical Geography*, 29(1), 104–113. <https://doi.org/10.1191/030913305PP437PR>
- Bakka, H., Rue, H., Fuglstad, G.-A., Riebler, A., Bolin, D., Illian, J., Krainski, E., Simpson, D., & Lindgren, F. (2018). Spatial modelling with R-INLA: A review. *Wiley Interdisciplinary Reviews: Computational Statistics*, 10(6). <https://doi.org/10.1002/WICS.1443>
- Beamish, A., Raynolds, M. K., Epstein, H., Frost, G. V., Macander, M. J., Bergstedt, H., Bartsch, A., Kruse, S., Miles, V., Tanis, C. M., Heim, B., Fuchs, M., Chabrillat, S., Shevtsova, I., Verdonen, M., & Wagner, J. (2020). Recent trends and remaining challenges for optical remote sensing of Arctic tundra vegetation: A review and outlook. *Remote Sensing of Environment*, 246, 111872. <https://doi.org/10.1016/J.RSE.2020.111872>
- Bjorkman, A. D., García Criado, M., Myers-Smith, I. H., Ravolainen, V., Jónsdóttir, I. S., Westergaard, K. B., Lawler, J. P., Aronsson, M., Bennett, B., Gardfjell, H., Heiðmarsson, S., Stewart, L., & Normand, S. (2020). Status and trends in Arctic vegetation: Evidence from experimental warming and long-term monitoring. *Ambio*, 49(3), 678–692. <https://doi.org/10.1007/S13280-019-01161-6>
- Ceballos, A., Hernández, J., Corvalán, P., & Galleguillos, M. (2015). Comparison of airborne LiDAR and satellite hyperspectral remote sensing to estimate vascular plant richness in deciduous Mediterranean forests of Central Chile. *Remote Sensing*, 7(3), 2692–2714. <https://doi.org/10.3390/RS70302692>
- Chadburn, S. E., Burke, E. J., Cox, P. M., Friedlingstein, P., Hugelius, G., & Westermann, S. (2017). An observation-based constraint on permafrost loss as a function of global warming. *Nature Climate Change*, 7(5), 340–344. <https://doi.org/10.1038/nclimate3262>
- Copernicus Sentinel-2 (processed by ESA). (2021). *MSI Level-2A BOA Reflectance Product. Collection 0*. European Space Agency. https://doi.org/10.5270/S2_-6eb6imz
- Crawley, M. J., & Harral, J. E. (2001). Scale dependence in plant biodiversity. *Science*, 291(5505), 864–868. <https://doi.org/10.1126/SCIENCE.291.5505.864>
- Criado, M. G., Myers-Smith, I. H., Bjorkman, A. D., Elmendorf, S. C., Normand, S., Aastrup, P., Aerts, R., Alatalo, J. M., Baeten, L., Björk, R. G., Björkman, M. P., Boulanger-Lapointe, N., Butler, E., Cooper, E. J., Cornelissen, J. H. C., Daskalova, G. N., Henry, G. H. R., Hollister, R. D., Høye, T. T., ... Vellend, M. (2023). *Plant diversity dynamics over space and time in a warming Arctic*. EcoEvoRxiv. <https://doi.org/10.32942/X2MS4N>
- Daniëls, F. J. a, Gillespie, L. J., Poulin, M., Afonina, O. M., Alsos, I. G., Aronsson, M., Bültmann, H., Ickert-bond, S., Konstantinova, N. a, Lovejoy, C., Väre, H., & Westergaard, K. B. (2013). Plants. In *Arctic Biodiversity Assessment* (pp. 310–353).
- Dearborn, K. D., & Danby, R. K. (2017). Aspect and slope influence plant community composition more than elevation across forest–tundra ecotones in subarctic Canada. *Journal of Vegetation Science*, 28(3), 595–604. <https://doi.org/10.1111/jvs.12521>
- Descals, A., Gaveau, D. L. A., Verger, A., Sheil, D., Naito, D., & Peñuelas, J. (2022). Unprecedented fire activity above the Arctic Circle linked to rising temperatures. *Science*, 378(6619), 532–537.

<https://doi.org/10.1126/SCIENCE.ABN9768>

- Drusch, M., Del Bello, U., Carlier, S., Colin, O., Fernandez, V., Gascon, F., Hoersch, B., Isola, C., Laberinti, P., Martimort, P., Meygret, A., Spoto, F., Sy, O., Marchese, F., & Bargellini, P. (2012). Sentinel-2: ESA's optical high-resolution mission for GMES operational services. *Remote Sensing of Environment*, 120, 25–36. <https://doi.org/10.1016/J.RSE.2011.11.026>
- Elmendorf, S. C., Henry, G. H. R., Hollister, R. D., Fosaa, A. M., Gould, W. A., Hermanutz, L., Hofgaard, A., Jónsdóttir, I. I., Jorgenson, J. C., Lévesque, E., Magnusson, B., Molau, U., Myers-Smith, I. H., Oberbauer, S. F., Rixen, C., Tweedie, C. E., & Walker, M. (2015). Experiment, monitoring, and gradient methods used to infer climate change effects on plant communities yield consistent patterns. *Proceedings of the National Academy of Sciences of the United States of America*, 112(2), 448–452. <https://doi.org/10.1073/pnas.1410088112>
- Evans Jeffrey, M. M. (2021). *spatialEco*. <https://jeffreyevans.github.io/spatialEco/authors.html>
- Everson, D. A., & H. Boucher, D. (1998). Tree species-richness and topographic complexity along the riparian edge of the Potomac River. *Forest Ecology and Management*, 109(1–3), 305–314. [https://doi.org/10.1016/S0378-1127\(98\)00264-3](https://doi.org/10.1016/S0378-1127(98)00264-3)
- Fassnacht, F. E., Müllerová, J., Conti, L., Malavasi, M., & Schmidlein, S. (2022). About the link between biodiversity and spectral variation. *Applied Vegetation Science*, 25(1), e12643. <https://doi.org/10.1111/avsc.12643>
- Féret, J. B., & Asner, G. P. (2014). Mapping tropical forest canopy diversity using high-fidelity imaging spectroscopy. *Ecological Applications*, 24(6), 1289–1296. <https://doi.org/10.1890/13-1824.1>
- Féret, J. B., & de Boissieu, F. (2020). biodivMapR: An r package for α - and β -diversity mapping using remotely sensed images. *Methods in Ecology and Evolution*, 11(1), 64–70. <https://doi.org/10.1111/2041-210X.13310>
- Gamon, J. A., Wang, R., Gholizadeh, H., Zutta, B., Townsend, P. A., & Cavender-Bares, J. (2020). Consideration of scale in remote sensing of biodiversity. *Remote Sensing of Plant Biodiversity*, 425–447. https://doi.org/10.1007/978-3-030-33157-3_16
- Gao, B. C. (1996). NDWI—A normalized difference water index for remote sensing of vegetation liquid water from space. *Remote Sensing of Environment*, 58(3), 257–266. [https://doi.org/10.1016/S0034-4257\(96\)00067-3](https://doi.org/10.1016/S0034-4257(96)00067-3)
- Gastauer, M., Nascimento, W. R., Caldeira, C. F., Ramos, S. J., Souza-Filho, P. W. M., & Féret, J. B. (2022). Spectral diversity allows remote detection of the rehabilitation status in an Amazonian iron mining complex. *International Journal of Applied Earth Observation and Geoinformation*, 106, 102653. <https://doi.org/10.1016/J.IJAG.2021.102653>
- GDAL/OGR contributors. (2023). *GDAL/OGR Geospatial data abstraction software library*. <https://doi.org/10.5281/zenodo.5884351>
- Gholizadeh, H., Gamon, J. A., Helzer, C. J., Cavender-Bares, J., Gholizadeh, C. ;, Gamon, J. A., Helzer, C. J., & Cavender, J. (2020). Multi-temporal assessment of grassland α - and β -diversity using hyperspectral imaging. *Ecological Applications*, 30(7), e02145. <https://doi.org/10.1002/EAP.2145>
- Grosse, G., Goetz, S., McGuire, A. D., Romanovsky, V. E., & Schuur, E. A. G. (2016). Changing permafrost in a warming world and feedbacks to the Earth system. *Environmental Research Letters*, 11(4), 040201. <https://doi.org/10.1088/1748-9326/11/4/040201>
- He, Z., Zhao, W., Chang, X., Chang, X., & Fang, J. (2006). Scale dependence in desert plant diversity.

Biodiversity and Conservation, 15(9), 3055–3064. <https://doi.org/10.1007/S10531-005-5396-7>

- Heim, R. J., Bucharova, A., Brodt, L., Kamp, J., Rieker, D., Soromotin, A. V., Yurtaev, A., & Hölzel, N. (2021). Post-fire vegetation succession in the Siberian subarctic tundra over 45 years. *Science of the Total Environment*, 760. <https://doi.org/10.1016/J.SCITOTENV.2020.143425>
- Henry, G. H. R., Hollister, R. D., Klanderud, K., Björk, R. G., Bjorkman, A. D., Elphinstone, C., Jónsdóttir, I. S., Molau, U., Petraglia, A., Oberbauer, S. F., Rixen, C., & Wookey, P. A. (2022). The International Tundra Experiment (ITEX): 30 years of research on tundra ecosystems. *Arctic Science*, 8(3), 550–571. <https://doi.org/10.1139/as-2022-0041>
- Ims, R. A., Ehrlich, D., Forbes, B. C., Huntley, B., Walker, D. A., Wookey, P. A., Berteaux, D., Bhatt, U. S., Bråthen, K. A., Edwards, M. E., Epstein, H. E., Forchhammer, M. C., Fuglei, E., Gauthier, G., Gilbert, S., Leung, M., Menyushina, I. E., Ovsyanikov, N., Post, E., ... van der Wal, R. (2013). Terrestrial Ecosystems - Arctic biodiversity, Conservation of Arctic Flora and Fauna (CAFF). In D. P. Hans Meltofte, Alf B. Josefson (Ed.), *Arctic biodiversity assessment : status and trends in Arctic biodiversity* (pp. 384–440). <https://www.arcticbiodiversity.is/the-report/chapters/terrestrial-ecosystems>
- Iturrate-Garcia, M., O'Brien, M. J., Khitun, O., Abiven, S., Niklaus, P. A., & Schaeppman-Strub, G. (2016). Interactive effects between plant functional types and soil factors on tundra species diversity and community composition. *Ecology and Evolution*, 6(22), 8126–8137. <https://doi.org/10.1002/ECE3.2548>
- Jaskólski, M. W. (2021). Challenges and perspectives for human activity in Arctic coastal environments - a review of selected interactions and problems. *Miscellanea Geographica*, 25(2), 127–143. <https://doi.org/10.2478/MGRSD-2020-0036>
- Jedrzejek, B., Drees, B., Daniëls, F. J. A., & Hölzel, N. (2013). Vegetation pattern of mountains in West Greenland – a baseline for long-term surveillance of global warming impacts. *Plant Ecology & Diversity*, 6(3–4), 405–422. <https://doi.org/10.1080/17550874.2013.802049>
- Kishore, B. S. P. C., Kumar, A., Saikia, P., & Khan, M. L. (2023). Alpha and beta diversity mapping in Indian tropical deciduous forests using high-fidelity imaging spectroscopy. *Advances in Space Research*. <https://doi.org/10.1016/J.ASR.2023.02.031>
- Kruschke, J. K. (2018). Rejecting or accepting parameter values in Bayesian estimation. *Advances in Methods and Practices in Psychological Science*, 17. <https://doi.org/10.1177/2515245918771304>
- Liaw, A., & Wiener, M. (2002). Classification and regression by randomForest. *R News*, 2(3). <http://www.stat.berkeley.edu/>
- Liccari, F., Sigura, M., & Bacaro, G. (2022). Use of remote sensing techniques to estimate plant diversity within ecological networks: A worked example. *Remote Sensing*, 14(19), 4933. <https://doi.org/10.3390/RS14194933/S1>
- Lundholm, J. T. (2009). Plant species diversity and environmental heterogeneity: spatial scale and competing hypotheses. *Journal of Vegetation Science*, 20(3), 377–391. <https://doi.org/10.1111/J.1654-1103.2009.05577.X>
- Main-Knorn, M., Pflug, B., Louis, J., Debaecker, V., Müller-Wilm, U., Magdalena Main-Knorn, A., & Gascon, F. (2017). Sen2Cor for Sentinel-2. *Proceedings of the SPIE*, 10427(4), 37–48. <https://doi.org/10.1117/12.2278218>
- McCrystall, M. R., Stroeve, J., Serreze, M., Forbes, B. C., & Screen, J. A. (2021). New climate models reveal faster and larger increases in Arctic precipitation than previously projected. *Nature*

Communications, 12(1), 1–12. <https://doi.org/10.1038/s41467-021-27031-y>

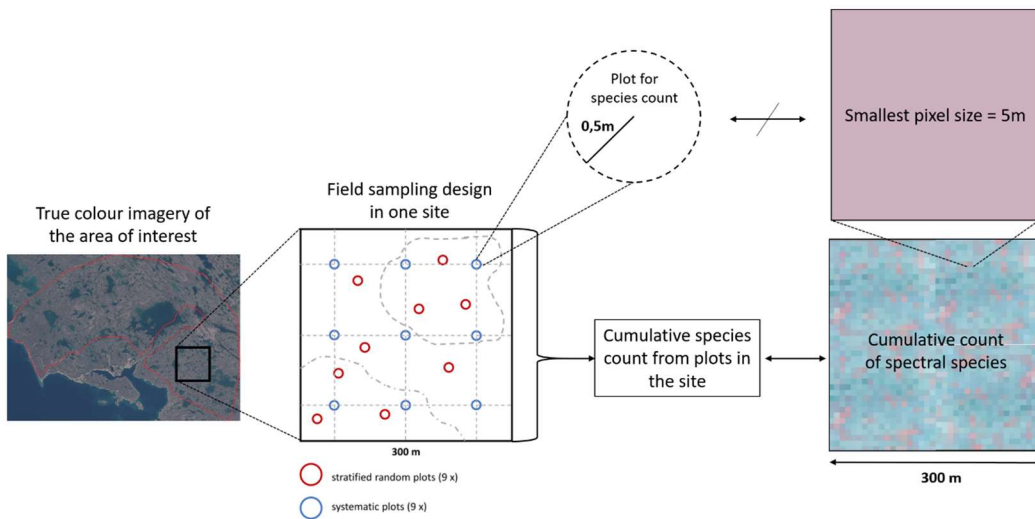
- McKane, R. B., Johnson, L. C., Shaver, G. R., Nadelhoffer, K. J., Rastetter, E. B., Fry, B., Giblin, A. E., Kielland, K., Kwiatkowski, B. L., Laundre, J. A., & Murray, G. (2002). Resource-based niches provide a basis for plant species diversity and dominance in arctic tundra. *Nature*, 415(6867), 68–71. <https://doi.org/10.1038/415068a>
- Metcalfe, D. B., Hermans, T. D. G., Ahlstrand, J., Becker, M., Berggren, M., Björk, R. G., Björkman, M. P., Blok, D., Chaudhary, N., Chisholm, C., Classen, A. T., Hasselquist, N. J., Jonsson, M., Kristensen, J. A., Kumordzi, B. B., Lee, H., Mayor, J. R., Prevéy, J., Pantazatou, K., ... Abdi, A. M. (2018). Patchy field sampling biases understanding of climate change impacts across the Arctic. *Nature Ecology & Evolution*, 2(9), 1443–1448. <https://doi.org/10.1038/s41559-018-0612-5>
- Michela, P., Mirko, D. F., Luisa, C., Jan, D., Milan, C., Petr, K., Laura, C. M., Duccio, R., Michele, T., Vítězslav, M., Petra, Š., Dominika, P., Jana, M., Jan, W., & Marco, M. (2023). The relationship between spectral and plant diversity: disentangling the influence of metrics and habitat types. *Remote Sensing of Environment*, 293. <https://doi.org/10.1101/2022.09.05.506583>
- Miller, C. E., Green, R. O., Thompson, D. R., Thorpe, A. K., Eastwood, M., Mccubbin, I. B., Olson-Duvall, W., Bernas, M., Sarture, C. M., Nolte, S., Rios, L. M., Hernandez, M. A., Bue, B. D., & Lundein, S. R. (2022). *ABoVE: Hyperspectral imagery AVIRIS-NG, Alaskan and Canadian Arctic, 2017-2019 V2*. ORNL Distributed Active Archive Center. <https://doi.org/10.3334/ORNLDAC/2009>
- Mod, H. K., Heikkinen, R. K., le Roux, P. C., Väre, H., & Luoto, M. (2016). Contrasting effects of biotic interactions on richness and distribution of vascular plants, bryophytes and lichens in an arctic-alpine landscape. *Polar Biology*, 39(4), 649–657. <https://doi.org/10.1007/S00300-015-1820-Y>
- Murray, D. F. (1995). Causes of Arctic plant diversity: Origin and evolution. In *Arctic and Alpine biodiversity: Patterns, causes and ecosystem consequences* (pp. 21–32). Springer, Berlin, Heidelberg. https://doi.org/10.1007/978-3-642-78966-3_2
- Myers-Smith, I. H., Kerby, J. T., Phoenix, G. K., Bjerke, J. W., Epstein, H. E., Assmann, J. J., John, C., Andreu-Hayles, L., Angers-Blondin, S., Beck, P. S. A., Berner, L. T., Bhatt, U. S., Bjorkman, A. D., Blok, D., Bryn, A., Christiansen, C. T., Cornelissen, J. H. C., Cunliffe, A. M., Elmendorf, S. C., ... Wipf, S. (2020). Complexity revealed in the greening of the Arctic. *Nature Climate Change*, 10(2), 106–117. <https://doi.org/10.1038/s41558-019-0688-1>
- Nelson, P. R., Maguire, A. J., Pierrat, Z., Orcutt, E. L., Yang, D., Serbin, S., Frost, G. V., Macander, M. J., Magney, T. S., Thompson, D. R., Wang, J. A., Oberbauer, S. F., Zesati, S. V., Davidson, S. J., Epstein, H. E., Unger, S., Campbell, P. K. E., Carmon, N., Velez-Reyes, M., & Huemmrich, K. F. (2021). Remote sensing of tundra ecosystems using high spectral resolution reflectance: Opportunities and challenges. *Journal of Geophysical Research: Biogeosciences*, 127(2). <https://doi.org/10.1029/2021JG006697>
- Niskanen, A., Heikkinen, R. K., Väre, H., & Luoto, M. (2017). Drivers of high-latitude plant diversity hotspots and their congruence. *Biological Conservation*, 212, 288–299. <https://doi.org/10.1016/J.BIOCON.2017.06.019>
- Niskanen, A., Luoto, M., Väre, H., & Heikkinen, R. K. (2017). Models of Arctic-alpine refugia highlight importance of climate and local topography. *Polar Biology*, 40(3), 489–502. <https://doi.org/10.1007/S00300-016-1973-3>
- Olofsson, J., te Beest, M., & Ericson, L. (2013). Complex biotic interactions drive long-term vegetation dynamics in a subarctic ecosystem. *Philosophical Transactions of the Royal Society of London. Series B, Biological Sciences*, 368(1624). <https://doi.org/10.1098/RSTB.2012.0486>

- Palmer, M. W., Earls, P. G., Hoagland, B. W., White, P. S., & Wohlgemuth, T. (2002). Quantitative tools for perfecting species lists. *Environmetrics*, 13(2), 121–137.
<https://doi.org/10.1002/ENV.516>
- Phiri, D., Simwanda, M., Salekin, S., Nyirenda, V. R., Murayama, Y., & Ranagalage, M. (2020). Sentinel-2 data for land cover/use mapping: A review. *Remote Sensing*, 12(14), 2291.
<https://doi.org/10.3390/RS12142291>
- Polyakova, M. A., Dembicz, I., Becker, T., Becker, U., Demina, O. N., Ermakov, N., Filibeck, G., Guarino, R., Janišová, M., Jaunatre, R., Kozub, Ł., Steinbauer, M. J., Suzuki, K., & Dengler, J. (2016). Scale- and taxon-dependent patterns of plant diversity in steppes of Khakassia, South Siberia (Russia). *Biodiversity and Conservation*, 25(12), 2251–2273. <https://doi.org/10.1007/S10531-016-1093-Y>
- Ponomarenko, S., McLennan, D., Pouliot, D., & Wagner, J. (2019). High resolution mapping of tundra ecosystems on Victoria Island, Nunavut – Application of a standardized terrestrial ecosystem classification. *Canadian Journal of Remote Sensing*, 45(5), 551–571.
<https://doi.org/10.1080/07038992.2019.1682980>
- Porter, C., Howat, I., Noh, M.-J., Husby, E., Khuvis, S., Danish, E., Tomko, K., Gardiner, J., Negrete, A., Yadav, B., Klassen, J., Kelleher, C., Cloutier, M., Bakker, J., Enos, J., Arnold, G., Bauer, G., & Morin, P. (2023). *ArcticDEM - Mosaics, Version 4.1*. Harvard Dataverse.
<https://doi.org/10.7910/DVN/3VDC4W>
- Qian, S. E. (2021). Hyperspectral satellites, evolution, and development history. *IEEE Journal of Selected Topics in Applied Earth Observations and Remote Sensing*, 14, 7032–7056.
<https://doi.org/10.1109/JSTARS.2021.3090256>
- Rantanen, M., Karpechko, A. Y., Lipponen, A., Nordling, K., Hyvärinen, O., Ruosteenoja, K., Vihma, T., & Laaksonen, A. (2022). The Arctic has warmed nearly four times faster than the globe since 1979. *Communications Earth & Environment*, 3(1), 1–10. <https://doi.org/10.1038/s43247-022-00498-3>
- Rast, M., Nieke, J., Adams, J., Isola, C., & Gascon, F. (2021). Copernicus Hyperspectral Imaging Mission for the Environment (Chime). *International Geoscience and Remote Sensing Symposium (IGARSS)*, 108–111. <https://doi.org/10.1109/IGARSS47720.2021.9553319>
- Rissanen, T., Aalto, A., Kainulainen, H., Kauppi, O., Niittynen, P., Soininen, J., & Luoto, M. (2023). Local snow and fluvial conditions drive taxonomic, functional and phylogenetic plant diversity in tundra. *Oikos*, 2023(10), e09998. <https://doi.org/10.1111/OIK.09998>
- Rocchini, D., Santos, M. J., Ustin, S. L., Féret, J.-B., Asner, G. P., & Beierkuhnlein, C. (2022). The spectral species concept in living color. *Journal of Geophysical Research*, 127.
<https://doi.org/10.1029/2022JG007026>
- Rocchini, D., Torresani, M., Beierkuhnlein, C., Feoli, E., Foody, G. M., Lenoir, J., Malavasi, M., Moudrý, V., Šimová, P., & Ricotta, C. (2022). Double down on remote sensing for biodiversity estimation: a biological mindset. *Community Ecology*, 23(3), 267–276. <https://doi.org/10.1007/S42974-022-00113-7>
- Rossi, C., Kneubühler, M., Schütz, M., Schaepman, M. E., Haller, R. M., & Risch, A. C. (2022). Spatial resolution, spectral metrics and biomass are key aspects in estimating plant species richness from spectral diversity in species-rich grasslands. *Remote Sensing in Ecology and Conservation*, 8(3), 297–314. <https://doi.org/10.1002/RSE2.244>
- Rossi, C., Kneubühler, M., Schütz, M., Schaepman, M. E., Haller, R. M., Risch, A. C., Rossi, C., Kneubühler, M., Schütz, M., Schaepman, M. E., & Haller, R. M. (2021). Remote sensing of

- spectral diversity: A new methodological approach to account for spatio-temporal dissimilarities between plant communities. *Ecological Indicators*, 130, 1470–160.
<https://doi.org/10.1016/j.ecolind.2021.108106>
- Rue, H., Riebler, A., Sørbye, S. H., Illian, J. B., Simpson, D. P., & Lindgren, F. K. (2017). Bayesian Computing with INLA: A Review. <Https://Doi.Org/10.1146/Annurev-Statistics-060116-054045>, 4, 395–421. <https://doi.org/10.1146/ANNUREV-STATISTICS-060116-054045>
- Runge, C., Daigle, R., & Hausner, V. (2020). Quantifying tourism booms and the increasing footprint in the Arctic with social media data. *PLoS ONE*, 15(1).
<https://doi.org/10.1371/journal.pone.0227189>
- Saarela, J. M., Sokoloff, P. C., Gillespie, L. J., Bull, R. D., Bennett, B. A., & Ponomarenko, S. (2020). Vascular plants of Victoria Island (Northwest Territories and Nunavut, Canada): a specimen-based study of an Arctic flora. *PhytoKeys* 141: 1-330, 141, 1–330.
<https://doi.org/10.3897/PHYTOKEYS.141.48810>
- Schmidlein, S., & Fassnacht, F. E. (2017). The spectral variability hypothesis does not hold across landscapes. *Remote Sensing of Environment*, 192, 114–125.
<https://doi.org/10.1016/J.RSE.2017.01.036>
- Schweiger, A. K., Cavender-Bares, J., Townsend, P. A., Hobbie, S. E., Madritch, M. D., Wang, R., Tilman, D., & Gamon, J. A. (2018). Plant spectral diversity integrates functional and phylogenetic components of biodiversity and predicts ecosystem function. *Nature Ecology & Evolution* 2018 2:6, 2(6), 976–982. <https://doi.org/10.1038/s41559-018-0551-1>
- Shaver, G. R., Laundre, J. A., Giblin, A. E., & Nadelhoffer, K. J. (1996). Changes in live plant biomass, primary production, and species composition along a riverside toposequence in Arctic Alaska. *Arctic and Alpine Research*, 28(3), 363–379. <https://doi.org/10.1080/00040851.1996.12003189>
- SK, S., & S, A. (2024). Exploring the advancements in high-performance computing paradigm for remote sensing big data analytics. *Cloud Computing and Data Science*, 5(1), 50–61.
<https://doi.org/10.37256/CCDS.5120243480>
- Stein, A., Gerstner, K., & Kreft, H. (2014). Environmental heterogeneity as a universal driver of species richness across taxa, biomes and spatial scales. *Ecology Letters*, 17(7), 866–880.
<https://doi.org/10.1111/ELE.12277>
- Stewart, L., Simonsen, C. E., Svenning, J. C., Schmidt, N. M., & Pellissier, L. (2018). Forecasted homogenization of high Arctic vegetation communities under climate change. *Journal of Biogeography*, 45(11), 2576–2587. <https://doi.org/10.1111/JBI.13434>
- Strong, L. W. (2016). Biased richness and evenness relationships within Shannon–Wiener index values. *Ecological Indicators*, 67, 703–713. <https://doi.org/10.1016/J.ECOLIND.2016.03.043>
- Tamme, R., Hiiesalu, I., Laanisto, L., Szava-Kovats, R., & Pärtel, M. (2010). Environmental heterogeneity, species diversity and co-existence at different spatial scales. *Journal of Vegetation Science*, 21(4), 796–801. <https://doi.org/10.1111/J.1654-1103.2010.01185.X>
- Tolvanen, A., Eilu, P., Juutinen, A., Kangas, K., Kivinen, M., Markovaara-Koivisto, M., Naskali, A., Salokannel, V., Tuulentie, S., & Similä, J. (2019). Mining in the Arctic environment – A review from ecological, socioeconomic and legal perspectives. *Journal of Environmental Management*, 233, 832–844. <https://doi.org/10.1016/J.JENVMAN.2018.11.124>
- Tsamba, J., Roux, P. le, Pertierra, L., Kuhlase, B., & Greve, M. (2023). Effect of grain size on patterns and drivers of plant species richness on a sub-Antarctic island. *Authorea Preprints*.
<https://doi.org/10.22541/AU.169660856.65660335/V1>

- Van Cleemput, E., Adler, P., & Suding, K. N. (2023). Making remote sense of biodiversity: What grassland characteristics make spectral diversity a good proxy for taxonomic diversity? *Global Ecology and Biogeography*, 1–12. <https://doi.org/10.1111/GEB.13759>
- Virkkala, A. M., Abdi, A. M., Luoto, M., & Metcalfe, D. B. (2019). Identifying multidisciplinary research gaps across Arctic terrestrial gradients. *Environmental Research Letters*, 14(12), 124061. <https://doi.org/10.1088/1748-9326/AB4291>
- Vollenweider, X., Bosco, C., Sánchez, R., & Tejerina, L. (n.d.). *High-resolution spatial modelling of population welfare in El Salvador, a coding tutorial*. Retrieved October 29, 2023, from <https://el-bid.github.io/tutorial-spatial-modelling-population-welfare-SCL-SPH/>
- Walker, D. A., Reynolds, M. K., Daniëls, F. J. A., Einarsson, E., Elvebakk, A., Gould, W. A., Katenin, A. E., Kholod, S. S., Markon, C. J., Melnikov, E. S., Moskalenko, N. G., Talbot, S. S., Yurtsev, B. A., Bliss, L. C., Edlund, S. A., Zoltai, S. C., Wilhelm, M., Bay, C., Gudjónsson, G., ... Vairin, B. A. (2005). The Circumpolar Arctic vegetation map. *Journal of Vegetation Science*, 16(3), 267–282. <https://doi.org/10.1111/J.1654-1103.2005.TB02365.X>
- Walker, M. D. (1995). Patterns and Causes of Arctic Plant Community Diversity. In *Arctic and Alpine Biodiversity: Patterns, Causes and Ecosystem Consequences* (pp. 3–20). https://doi.org/10.1007/978-3-642-78966-3_1
- Walker, Marilyn D., Gould, W. A., & Chapin, F. S. (2001). Scenarios of biodiversity changes in Arctic and Alpine tundra. In *Global Biodiversity in a Changing Environment* (pp. 83–100). Springer, New York, NY. https://doi.org/10.1007/978-1-4613-0157-8_5
- Yang, D., Morrison, B. D., Davidson, K. J., Lamour, J., Li, Q., Nelson, P. R., Hantson, W., Hayes, D. J., Swetnam, T. L., McMahon, A., Anderson, J., Ely, K. S., Rogers, A., & Serbin, S. P. (2022). Remote sensing from unoccupied aerial systems: Opportunities to enhance Arctic plant ecology in a changing climate. *Journal of Ecology*, 110(12), 2812–2835. <https://doi.org/10.1111/1365-2745.13976>
- Yu, F., Wang, T., Groen, T. A., Skidmore, A. K., Yang, X., Geng, Y., & Ma, K. (2015). Multi-scale comparison of topographic complexity indices in relation to plant species richness. *Ecological Complexity*, 22, 93–101. <https://doi.org/10.1016/J.ECOCOM.2015.02.007>
- Zhai, H., Zhang, H., Zhang, L., & Li, P. (2018). Cloud/shadow detection based on spectral indices for multi/hyperspectral optical remote sensing imagery. *ISPRS Journal of Photogrammetry and Remote Sensing*, 144, 235–253. <https://doi.org/10.1016/J.ISPRSJPRS.2018.07.006>
- Zhang, Y., Tang, J., Wu, Q., Huang, S., Yao, X., & Dong, J. (2023). Assessment of the capability of Landsat and BiodivMapR to track the change of alpha diversity in dryland disturbed by mining. *Remote. Sens.*, 15(6), 1554. <https://doi.org/10.3390/RS15061554>

Supplementary material



Supplementary Figure S1 : Illustration of the link between field data sampled this summer by members of the Spatial Ecology and Remote Sensing group and remote sensing data. The minimal pixel size is larger than the plot size, making the comparison of plot richness with richness estimate by remote sensing not possible. The comparison can take place between site richness, calculated as a cumulative sum of the 18 plots species richness, and the spectral species cumulative count for the corresponding area. The illustration proportions are not accurate.

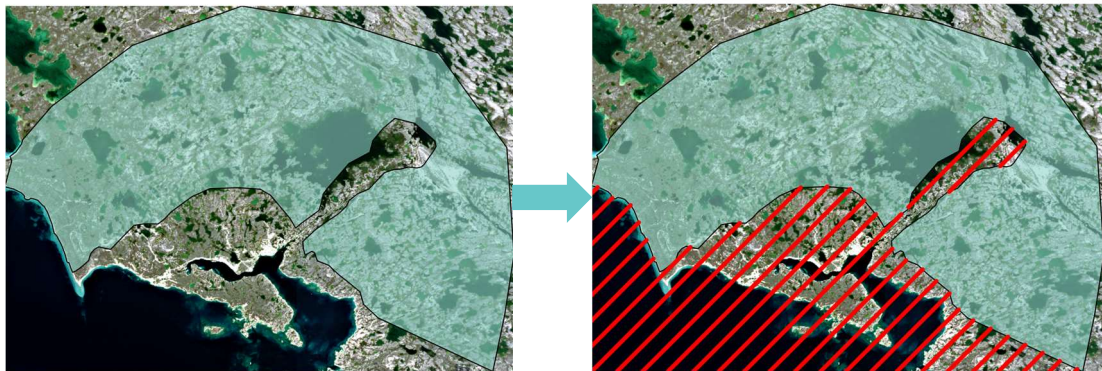
Supplementary Table S1: Species list of vegetation (vascular plant, mosses and lichen species) found at the three fieldwork sites visited by members of the Spatial Ecology and Remote Sensing group of the Zürich University during the summer 2023 (1.Bridge site, 2. Ovayok, 3. Long Point). Each sites spanned 300 by 300 m and contained 18 subplots. The numbers in the columns Site 1, Site 2, Site 3 corresponds to the number of subplots in which a plant species was found present.

species	Site 1	Site 2	Site 3
Arctagrostis latifolia (R.Br.) Griseb. subsp. latifolia	1	0	0
Astragalus alpinus L.	0	0	2
Bistorta vivipara (L.) Delarbre	11	11	14
Cardamine digitata Richardson	0	0	2
Carex aquatilis subsp. stans (Drejer) Hultén	2	1	3
Carex atrofusca Schkuhr	1	1	1
Carex bigelowii Torr. ex Schwein.	1	0	0
Carex borealipolaris S.R.Zhang	0	1	1
Carex capillaris subsp. fuscidula (V.I.Krecz. ex T.V.Egorova) Á.Löve &	1	0	0
Carex marina Dewey	2	0	1
Carex membranacea Hook.	1	6	10
Carex myosuroides Vill.	1	0	0
Carex rupestris All.	12	13	10
Carex scirpoidea Michx. subsp. scirpoidea	8	8	3
Carex simpliciuscula subsp. subholarctica (T.V.Egorova) Saarela	2	3	3

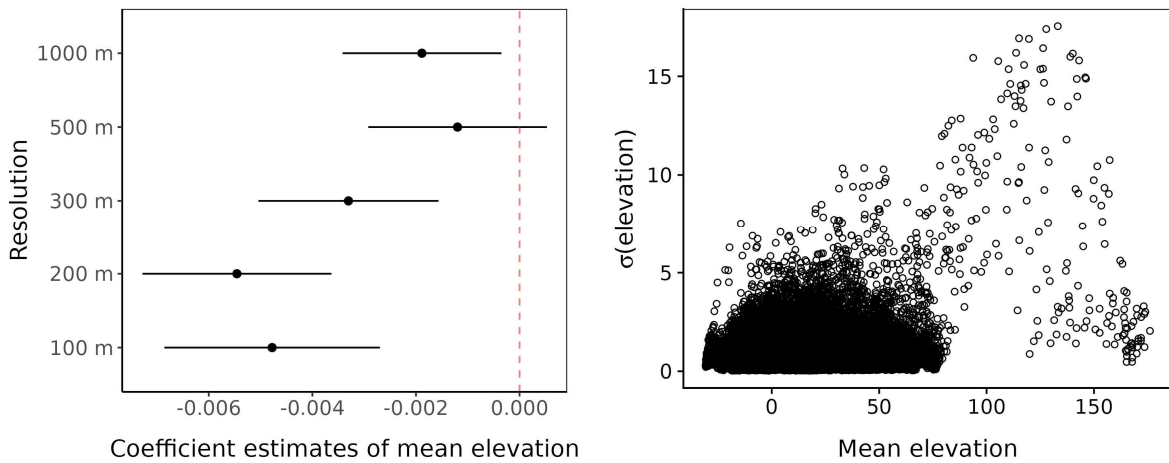
species	Site 1	Site 2	Site 3
<i>Carex vaginata</i> Tausch	0	0	1
<i>Cassiope tetragona</i> (L.) D.Don subsp. <i>tetragona</i>	0	0	4
<i>Chamaenerion latifolium</i> (L.) Sweet	0	3	3
<i>Draba lactea</i> Adams	0	1	0
<i>Draba nivalis</i> Lilj.	1	0	0
<i>Dryas integrifolia</i> Vahl subsp. <i>integrifolia</i>	16	17	16
<i>Dupontia fisheri</i> R.Br.	0	0	1
<i>Equisetum arvense</i> subsp. <i>alpestre</i> (Wahlenb.) Schonswetter &	0	0	1
<i>Equisetum variegatum</i> Schleich. ex F.Weber & D.Mohr subsp.	0	3	3
<i>Eriophorum angustifolium</i> Honck.	1	0	1
<i>Eriophorum triste</i> (Th.Fr.) Hadac & Á.Löve	0	0	2
<i>Hedysarum boreale</i> subsp. <i>mackenziei</i> (Richardson) S.L. Welsh	6	2	0
<i>Hulteniall integrifolia</i> (Richardson) Tzvelev	1	0	3
<i>Juncus biglumis</i> L.	0	1	1
<i>Juncus triglumis</i> subsp. <i>albescens</i> (Lange) Hultén	0	1	1
<i>Oxyria digyna</i> (L.) Hill	0	2	1
<i>Oxytropis arctobia</i> Bunge	5	5	1
<i>Oxytropis maydelliana</i> Trautv.	3	9	11
<i>Parrya arctica</i> R.Br.	2	0	0
<i>Pedicularis capitata</i> Adams	6	3	8
<i>Pedicularis lanata</i> Willd. ex Cham. & Schldl.	6	3	8
<i>Pedicularis langsdorffii</i> subsp. <i>arctica</i> (R.Br.) Pennell ex Hultén	1	0	1
<i>Physaria arctica</i> (Wormsk. ex Hornem.) O'Kane & Al-Shehbaz	3	7	0
<i>Sabulina rubella</i> (Wahlenb.) Dillenb. & Kadereit	0	0	1
<i>Salix arctica</i> Pall.	9	5	14
<i>Salix polaris</i> Wahlenb.	0	0	1
<i>Salix reticulata</i> L.	4	4	11
<i>Salix richardsonii</i> Hook.	3	2	5
<i>Saxifraga aizoides</i> L.	0	4	0
<i>Saxifraga cespitosa</i> L.	0	0	1
<i>Saxifraga oppositifolia</i> L.	9	13	11
<i>Saxifraga tricuspidata</i> Rottb.	1	0	0
<i>Silene uralensis</i> (Rupr.) Bocquet subsp. <i>uralensis</i>	0	2	0
<i>Tofieldia coccinea</i> Richardson	0	1	0
<i>Woodsia glabella</i> R.Br.	0	3	0

Supplementary Method S1: Detailed description of the field plant presence-absence sampling scheme, taken from Tundra eDNA Project Protocols by Jakob J. Assman and Debora Obrist (with their consent).

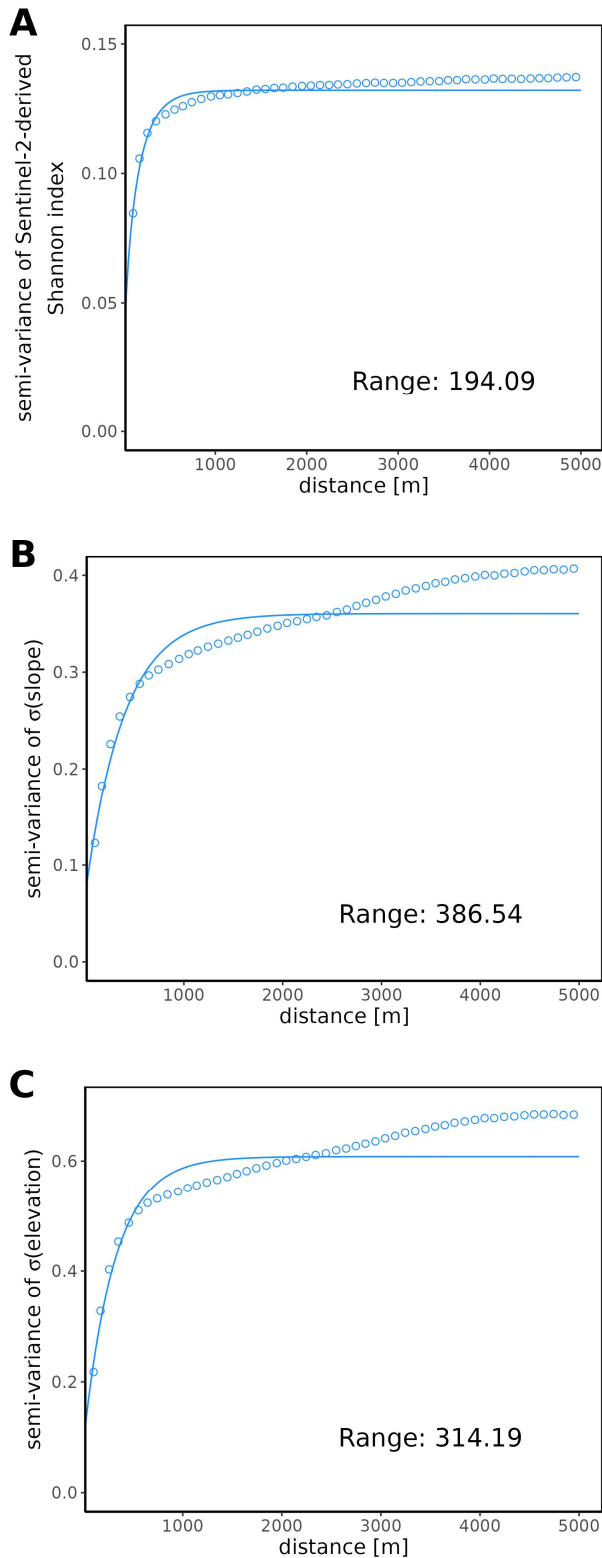
"We chose three research sites within 60 min travel from CHARS (approx. 20 km radius) and outside the 5 km radius of the Cambridge Bay airport. Travel to the research sites was facilitated by ATV and by foot. The three research sites were chosen so as to cover as much variety in the flora (vascular and moss). The three sites are: 1) Bridge site, 2) Ovayok, 3) Long Point. The dimension of each study site is 300 m x 300 m. We chose a preliminary centre for each site so that surrounding 300 m x 300 m (N-S, E-W) roughly cover the diversity of vegetation types present at the site. We then generate two random numbers (between -10 and +10) to "jitter" the preliminary site centre in N-S and E-W direction to reduce subconscious bias in the grid. We aimed to establish a total of 18 circular plots with 0.5 m radius in each study site. We tested two spatial sampling schemes an even geographic sampling versus a stratified random sampling. Systematic sampling: Nine plots were systematically in a square grid (100 m spacing; grid centre located on site centre). An excel spreadsheet was used to generate these coordinates automatically from the centre coordinates of the site (in UTM). We used a handheld Garmin GPS Map 66s to find the coordinates. Stratified random sampling: The remaining nine plots were placed (stratified) random. A rough visual assessment of the main cover types and vegetation communities at the site was done. The number of main cover types (3-6) and associated proportions covered of the whole site were approximated. An equal number of plots were assigned to each class. Where the number of classes was not an even divisor of nine, the remaining plots were assigned to the cover classes with the most cover - hierarchically from the top and one each class. To achieve the random sampling within each cover an excel spreadsheet was used to generate nine random locations within the site, based on the centre coordinate. The random coordinates were worked off one by one. We used a handheld Garmin GPS Map 66s to find the coordinates. If a random sample location fell within 10 m distance of an already sampled location (systematic or random) then it was discarded and a new coordinate generated. The same applied if the coordinate fell into water or on bare rock. At the location we noted down the main cover. Where the set proportion of plots in one cover type was reached we discarded any new coordinate that fell into this cover type picked the patch of the nearest different cover type not sufficiently sampled and walked to the centre of that patch in a straight line. Once we arrived at the patch, we did a random "jitter" to establish the location of the plot. This "jitter" was done by moving a random number of steps in the two main cardinal directions (N-S, and E-W). The number of steps was generated using a random number generator on a smartphone, choosing from a set of random numbers based on the estimated extent of the patch in N-S and E-W direction. We collected presence absence observation across the whole area of the 0.5 m radius circle. For this we used a string attached to two nails. We started in N-S and then moved the string clockwise. Each time the string intersected with a new plant species the identity was recorded. We started off doing both vascular plants and bryophytes at the same time, but later switched to doing vascular plants first then bryophytes. Where we could not determine the identity of a plant in the field we took a sample for later identification in the lab and placed it into a paper bag. As many bryophytes cannot be identified to species in the field, we identified the genus where we could and then took a sample of the specimen for confirmation and later identification. For logistical and damage reduction reasons we only sampled specimens of one genus if they were further apart than approximately 10 cm of an already sampled member of that genus. A comprehensive sampling of all bryophytes in the plot would have logically not been possible. We estimate that we captured about 70-90% of the moss genera present at the site by identification in the field. Moss genera were confirmed in the laboratory with the help of an expert (Erin Cox) afterwards."



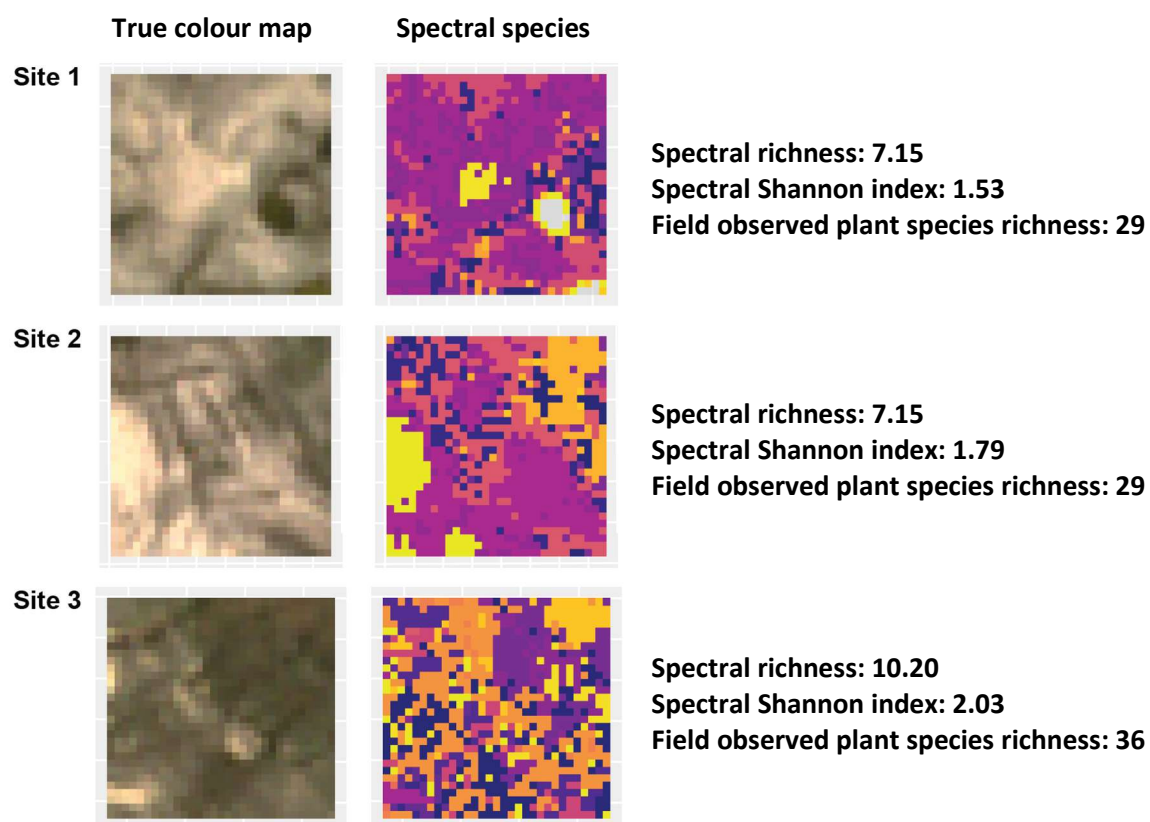
Supplementary Figure S2: true colour map of the extent of the area of interest communicated by Jakob J. Assmann, itself shown in pale blue (left). Red hatched area correspond to pixel that were mask for this study to remove built-up area from the analysis (right).



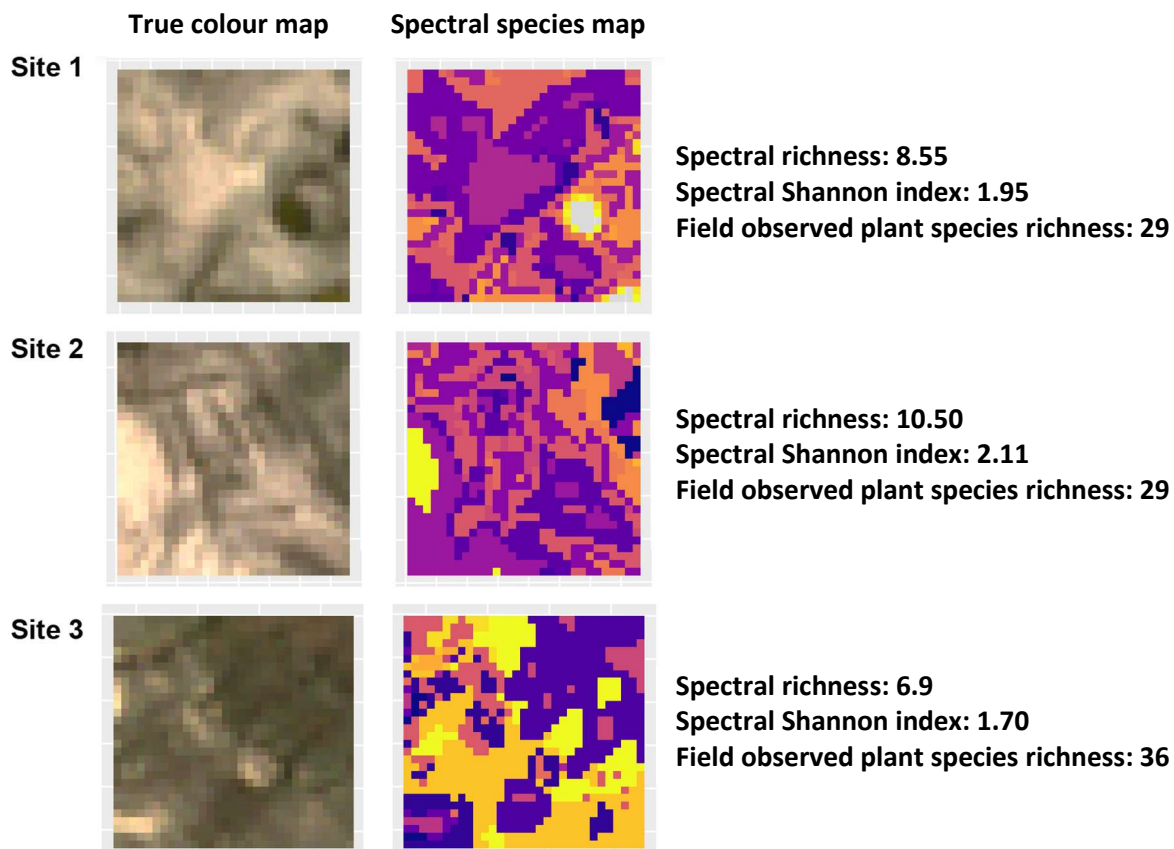
Supplementary Figure S3: Coefficient estimates for the standard deviation in elevation in model with Sentinel-2 derived spectral species diversity as response variable and standard deviation in elevation as predictor (left). The response variable and predictors where computed at 100 m, 200 m, 300 m, 500 m, and 1000 m resolution, to obtain as many model results. The right graph shows the relationship between mean elevation and standard deviation of elevation computed at 100 m resolution. Both results supported the computation of the coefficient of variation in elevation instead of the standard deviation in elevation.



Supplementary Figure S4: Semi-variograms of the 100 m resolution spectral species Shannon index derived from Sentinel-2 data (A), the standard deviation of slope (B) and the standard deviation of elevation (C). The semi-variograms were computed with an interval distance of 100 meters, corresponding to one pixel.



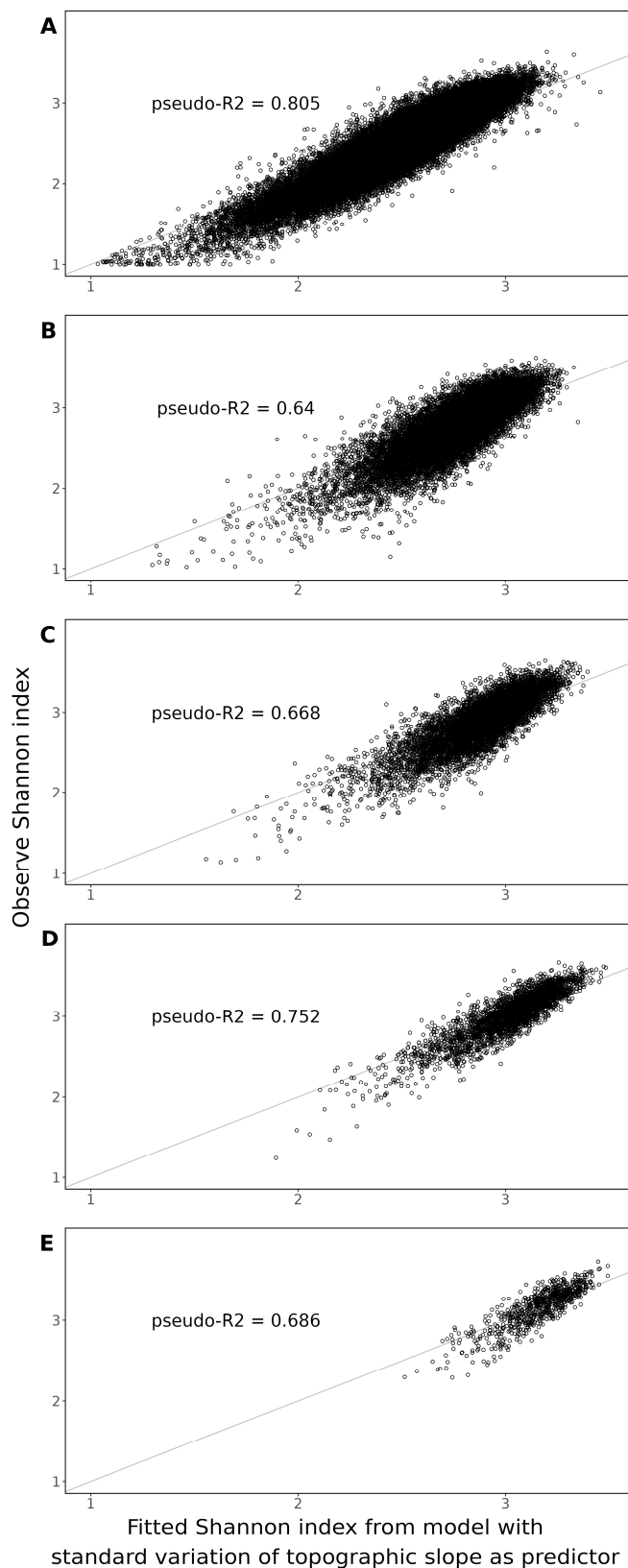
Supplementary Figure S5: Sentinel-2 derived spectral diversity computed for the fieldwork sites using spectral species map produced with principal components 1, 2, 7, and 8. Left: true colour maps of the fieldwork sites from Sentinel 2 satellite. Middle: Illustration of the pixel-assignment to the 20 spectral species for one of the 20 iterations, where each (arbitrary) colour corresponds to a spectral species. Right: Spectral richness, computed as the number of spectral species present the area of the site; spectral Shannon index, computed with the spectral richness and the abundance of each spectral species in the area of the site; and the field observed plant species richness, based on 18 plots in each site.



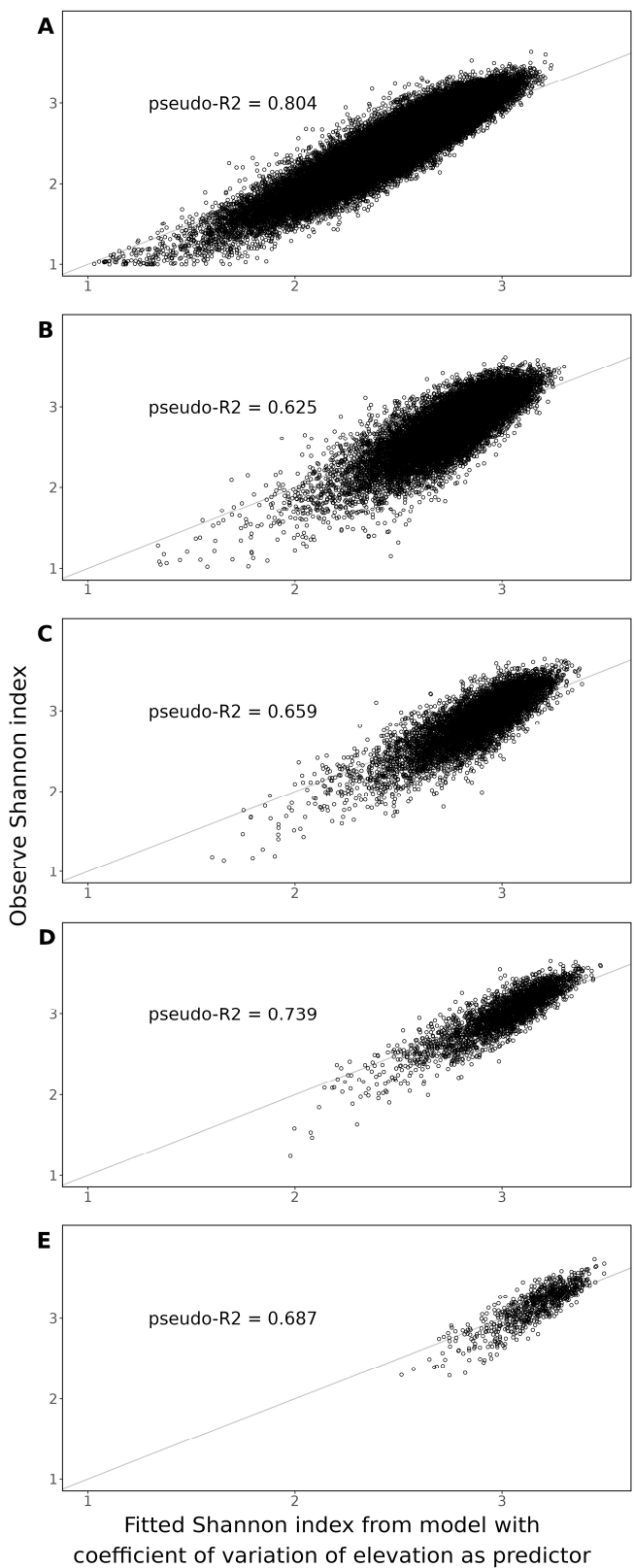
Supplementary Figure S6: Sentinel-2 derived spectral diversity computed for the fieldwork sites using spectral species map produced with principal components 1, 2, cumulatively explaining 94.5% of the variance. Left: true colour maps of the fieldwork sites from Sentinel 2 satellite. Middle: Illustration of the pixel-assignment to the 20 spectral species for one of the 20 iterations, where each (arbitrary) colour correspond to a spectral species. Right: Spectral richness, computed as the number of spectral species present the area of the site; spectral Shannon index, computed with the spectral richness and the abundance of each spectral species in the area of the site; and the field observed plant species richness, based on 18 plots in each site.

Supplementary Table S2: Coefficient table from models explaining spectral diversity (Shannon index), computed from Sentinel-2 data, with standard deviation of slope. Models account for autocorrelation in the spectral diversity as a random term and models output a range. Models were run at 100, 200, 300, 500, 1000 m resolution. Mean of the coefficients as well 2.5% and 97.5% percentile are displayed.

	sd(slope)			Range		
	mean	0.025	0.975	mean	0.025	0.975
100 m	0.044	0.041	0.046	3.930	3.792	4.102
200 m	0.025	0.022	0.028	5.659	5.121	6.192
300 m	0.016	0.012	0.019	6.109	5.325	7.056
500 m	0.013	0.008	0.018	5.361	4.434	6.502
1000 m	0.000	-0.008	0.007	6.073	3.937	9.448



Supplementary Figure S7: Sentinel-2 derived spectral species Shannon index values against the mean spectral species Shannon index values output from an INLA using the standard deviation of the topographic slope as predictor and a latent effect accounting for spatial autocorrelation. The fitted values are obtained by transforming the linear predictors by the inverse of the link function. Plot from A to E represents models using data at 100, 200, 300, 500 and 1000 m resolution respectively.



Supplementary Figure S8: Sentinel-2 derived spectral species Shannon index values against the mean spectral species Shannon index values output from an INLA using the coefficient of variation of elevation as predictor and a latent effect accounting for spatial autocorrelation. The fitted values are obtained by transforming the linear predictors by the inverse of the link function. Plot from A to E represents models using data at 100, 200, 300, 500 and 1000 m resolution respectively.

Supplementary Table S3: Coefficient table from models explaining spectral diversity (Shannon index), computed from Sentinel-2 data, with coefficient of variation (CV) of elevation. Models account for autocorrelation in the spectral diversity as a random term and models output a range. Models were run at 100, 200, 300, 500, 1000 m resolution. Mean of the coefficients as well 2.5% and 97.5% percentile are displayed.

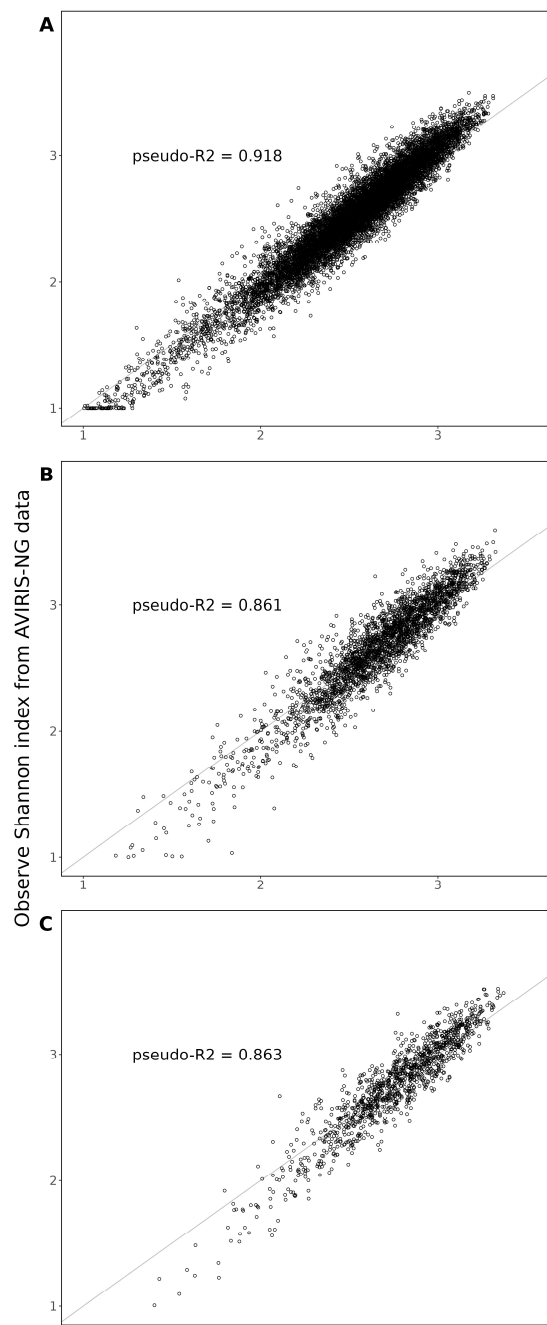
	CV(elevation)			Range		
	mean	0.025	0.975	mean	0.025	0.975
100 m	0	0.000	0.000	3.730	3.595	3.871
200 m	0	-0.001	0.000	5.483	4.977	6.021
300 m	0	0.000	0.000	5.981	5.188	6.885
500 m	0	-0.001	0.001	5.282	4.353	6.452
1000 m	0	0.000	0.000	6.019	3.927	9.382

Supplementary Table S4: Coefficients table from models explaining spectral diversity (Shannon index), computed one AVIRIS-NG flight strip, with standard deviation of slope. Models account for autocorrelation in the spectral diversity as a random term and models output a range. Models were run at 100, 200, 300, 500, 1000 m resolution. Mean of the coefficient of variation as well 2.5% and 97.5% percentile are displayed.

	sd(slope)			Range		
	mean	0.025	0.975	mean	0.025	0.975
100 m	0.036	0.028	0.044	6.703	6.101	7.359
200 m	0.021	0.007	0.035	6.905	5.692	8.405
300 m	0.012	-0.006	0.031	6.410	4.791	8.618

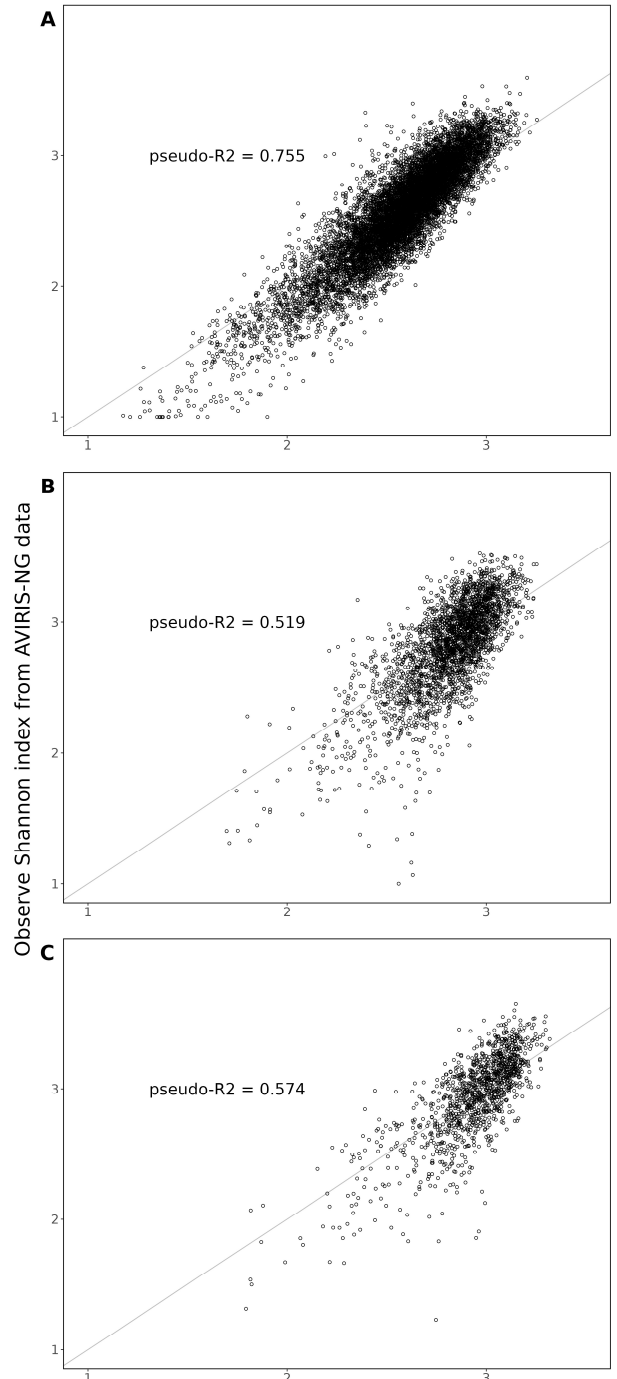
Supplementary Table S5: Coefficients table from models explaining spectral diversity (Shannon index), computed from Sentinel-2 data spanning one AVIRIS-NG flight strip extent, with standard deviation of slope. Models account for autocorrelation in the spectral diversity as a random term and models output a range. Models were run at 100, 200, 300, 500, 1000 m resolution. Mean of the coefficient of variation as well 2.5% and 97.5% percentile are displayed.

	sd(slope)			Range		
	mean	0.025	0.975	mean	0.025	0.975
100 m	0.055	0.046	0.064	4.514	4.079	4.992
200 m	0.018	0.006	0.031	10.300	7.577	14.106
300 m	-0.004	-0.020	0.013	13.672	9.139	20.921



Fitted Shannon index from AVIRIS-NG data, modelled with standard variation of topographic slope as predictor

Supplementary Figure S9: AVIRIS-NG derived spectral species Shannon index values against the mean spectral species Shannon index values output from an INLA using the standard deviation of the topographic slope as predictor and a latent effect accounting for spatial autocorrelation. The fitted values are obtained by transforming the linear predictors by the inverse of the link function. Plot from A to C represents models using data at 100, 200 and 300 m resolution respectively.



Fitted Shannon index from Sentinel-2 data, modelled with standard variation of topographic slope as predictor

Supplementary Figure S10: Sentinel-2 derived spectral species Shannon index values against the mean spectral species Shannon index values output from an INLA using the standard deviation of the topographic slope as predictor and a latent effect accounting for spatial autocorrelation. The fitted values are obtained by transforming the linear predictors by the inverse of the link function. Plot from A to C represents models using data at 100, 200 and 300 m resolution respectively.



Eidgenössische Technische Hochschule Zürich
Swiss Federal Institute of Technology Zurich

Declaration of originality

The signed declaration of originality is a component of every semester paper, Bachelor's thesis, Master's thesis and any other degree paper undertaken during the course of studies, including the respective electronic versions.

Lecturers may also require a declaration of originality for other written papers compiled for their courses.

I hereby confirm that I am the sole author of the written work here enclosed and that I have compiled it in my own words. Parts excepted are corrections of form and content by the supervisor.

Title of work (in block letters):

MAPPING OF SPECTRAL SPECIES DIVERSITY IN THE ARCTIC TUNDRA AND ITS
RELATIONSHIP WITH TOPOGRAPHIC COMPLEXITY - A USE CASE OF THE SPECTRAL
SPECIES CONCEPT IN BIODIVERSITY RESEARCH AND CONSERVATION

Authored by (in block letters):

For papers written by groups the names of all authors are required.

Name(s):

PIJNENBURG

First name(s):

MARIE-LOU

With my signature I confirm that

- I have committed none of the forms of plagiarism described in the 'Citation etiquette' information sheet.
- I have documented all methods, data and processes truthfully.
- I have not manipulated any data.
- I have mentioned all persons who were significant facilitators of the work.

I am aware that the work may be screened electronically for plagiarism.

Place, date

Zürich, the 13 of November 2023

Signature(s)

For papers written by groups the names of all authors are required. Their signatures collectively guarantee the entire content of the written paper.